

**UNIVERSIDADE FEDERAL DE SANTA MARIA
CENTRO DE CIÊNCIAS NATURAIS E EXATAS
PROGRAMA DE PÓS-GRADUAÇÃO EM QUÍMICA**

**PHYSICAL-CHEMICAL STUDY OF EFFECTS OF
FUNCTIONAL GROUPS ON ADSORPTION BEHAVIOR
OF NAPHTHALENE AND ITS DERIVATIVES ON HIGH-
DENSITY POLYETHYLENE MICROPLASTICS**

DISSERTAÇÃO DE MESTRADO

Ronaldo Antunes Funari Junior

Santa Maria, RS, Brasil

**PHYSICAL-CHEMICAL STUDY OF EFFECTS OF FUNCTIONAL
GROUPS ON ADSORPTION BEHAVIOR OF NAPHTHALENE
AND ITS DERIVATIVES ON HIGH-DENSITY POLYETHYLENE
MICROPLASTICS**

Por

RONALDO ANTUNES FUNARI JUNIOR

Dissertação apresentada ao Programa de pós-graduação em Química na área de concentração em Físico-Química da Universidade Federal de Santa Maria (RS), como requisito parcial para a obtenção do título de **Mestre em Ciências – Área de concentração: Físico-Química.**

SANTA MARIA, RS – BRASIL

Novembro de 2023

This study was financed in part by the Coordenação de Aperfeiçoamento de Pessoal de Nível Superior - Brasil (CAPES) - Finance Code 001

Funari, Ronaldo
Physical-Chemical Study of effects of functional groups on adsorption behavior of naphthlene and its derivatives on high-density polyethylene microplastics / Ronaldo Funari.- 2023.
66 p.; 30 cm

Orientador: Marcelo Barcellos da Rosa
Dissertação (mestrado) - Universidade Federal de Santa Maria, Centro de Ciências Naturais e Exatas, Programa de Pós-Graduação em Química, RS, 2023

1. Adsorption 2. Thermodynamic 3. Isotherm I.
Barcellos da Rosa, Marcelo II. Título.

Sistema de geração automática de ficha catalográfica da UFSM. Dados fornecidos pelo autor(a). Sob supervisão da Direção da Divisão de Processos Técnicos da Biblioteca Central. Bibliotecária responsável Paula Schoenfeldt Patta CRB 10/1728.

Declaro, RONALDO FUNARI, para os devidos fins e sob as penas da lei, que a pesquisa constante neste trabalho de conclusão de curso (Dissertação) foi por mim elaborada e que as informações necessárias objeto de consulta em literatura e outras fontes estão devidamente referenciadas. Declaro, ainda, que este trabalho ou parte dele não foi apresentado anteriormente para obtenção de qualquer outro grau acadêmico, estando ciente de que a inveracidade da presente declaração poderá resultar na anulação da titulação pela Universidade, entre outras consequências legais.

Agradecimentos

- Aos meus avós, Arlete e Vulmo, por serem essenciais na minha vida e sempre me apoiarem em tudo, amo vocês incondicionalmente.
- A minha mãe Mariglei e meu irmão Lutiano, essa conquista é para vocês também, e pela mana que está pra sempre conosco.
- A minha vó materna, Fátima, trabalhadora, guerreira, a quem tenho orgulho de ser neto.
- A todos os professores que fizeram parte da minha formação e me ensinaram muito mais que conteúdos, mas ajudaram a formar a pessoa e profissional que almejo ser.
- Ao meu orientador, Prof. Dr. Marcelo Barcellos da Rosa por toda ajuda durante esses dois anos de mestrado, pelo acolhimento dado mesmo vindo de outra instituição.
- A todos os colegas do LAQUIF, hoje amigos, que deram todo suporte necessário para o desenvolvimento deste trabalho.
- Ao Lucas e Bryan que agregaram muito na minha caminhada na pós-graduação, conselhos, conversas, ensinamentos sobre química e também muita risada com assuntos irrelevantes e de péssima procedência.
- Aos membros da banca examinadora, Prof. Dr. Guilherme Luiz Dotto, e Prof. Dr. Sérgio Roberto Mortari pelas contribuições com o trabalho.
- Aos professores do PPGQ, pelo conhecimento construído durante os créditos.
- A Coordenação de Aperfeiçoamento de Pessoal de Nível Superior – CAPES, pelo financiamento.

RESUMO

Título: Estudo físico-químico dos efeitos de grupos funcionais no comportamento de adsorção de naftaleno e seus derivados em microplásticos de polietileno de alta densidade

Autor: Ronaldo Antunes Funari Junior

Orientador: Prof. Dr. Marcelo Barcellos da Rosa

Os microplásticos (MP) têm recebido grande atenção devido aos resíduos produzidos em massa lançados no meio ambiente. MP são ideais para aderir a poluentes orgânicos que podem ser facilmente dispersos, oferecendo riscos à saúde humana. Além disso, pouco foi relatado sobre como diferentes grupos funcionais em derivados de hidrocarbonetos policíclicos aromáticos (HPA) influenciam o comportamento de adsorção em MP. Para entender melhor esse processo, os grupos metil ($-\text{CH}_3$) e hidroxila ($-\text{OH}$) foram selecionados e polietileno de alta densidade comercial e residual (PEAD, $\leq 1\text{mm}$) foram usados como adsorventes, e Naftaleno (Naf), 1-Metil-Naftaleno (Me-Naf) e α -Naftol como adsorvatos. Os resultados mostraram comportamentos diferentes para adsorvatos apolares e polares. Forças de dispersão foram o principal tipo de interação entre PEAD e Naf/Me-Naf, enquanto forças dipolo-induzidas e ligações de hidrogênio foram as principais interações envolvendo MP e compostos polares. Independente da fonte de PEAD, Naf e Me-Naf possuem isoterma Tipo III, e α -Naftol apresenta isoterma Tipo II. Naf e Me-Naf ajustados à isoterma de Freundlich com um processo desfavorável ($n = 2,12$ e $1,11$; $1,87$ e $1,31$, respectivamente), com valores positivos de ΔH° (50 e $77,17$; 66 e $64,63 \text{ kJ mol}^{-1}$) e ΔS° ($0,070$ e $0,0145$; $0,122$ e $0,103 \text{ kJ mol}^{-1}$) para MP comercial e de residual, respectivamente. Além disso, a isoterma de adsorção de α -Naftol em PEAD comercial e residual ajustada ao modelo de Langmuir ($Q_{max} = 42,5$ e $27,2 \mu\text{mol g}^{-1}$, respectivamente), apresentando valores negativos de ΔH° ($-43,71$ e $-44,10 \text{ kJ mol}^{-1}$) e ΔS° ($-0,037$ e $-0,025 \text{ kJ mol}^{-1}$). O estudo da cinética de adsorção apresenta um modelo não linear de pseudo-segunda ordem para todos os casos. Os valores de K_2 seguem a ordem Me-Naf > Naf > α -Naftol em ambos MP. Portanto, este estudo experimental fornece novos insights sobre a afinidade de derivados de HPA para uma classe específica de MP, ajudando a entender o destino ambiental de MP residual e poluentes orgânicos.

Palavras-chave: Microplásticos de PEAD, mecanismos de adsorção, derivados de Naf, grupos funcionais.

ABSTRACT

Title: Physical-chemical study of effects of functional groups on adsorption of naphthalene and its derivatives onto high-density polyethylene microplastics

Author: Ronaldo Antunes Funari Junior

Academic Advisor: Prof. Dr. Marcelo Barcellos da Rosa

Microplastics (MP) have received great attention due to the mass-produced residues discharged into the environment. MP are ideal for adhering to organic pollutants that can be easily dispersed, thus posing risks to human health. Furthermore, little has been reported on how different functional groups in polycyclic aromatic hydrocarbons (PAH) derivatives influence the adsorption behavior on MP. To better understand this process, groups methyl ($-\text{CH}_3$) and hydroxyl ($-\text{OH}$) were selected and commercial and waste high-density polyethylene (HDPE, $\leq 1\text{mm}$) were used as adsorbents, and Naphthalene (Nap), 1-Methyl-Naphthalene (Me-Nap) and α -Naphthol as adsorbates. The results showed different behaviors for nonpolar and polar adsorbates. Dispersion forces were the main type of interaction between HDPE and Nap/Me-Nap, while dipole-induced dipole forces and H-bonding were the chief interactions involving MP and polar compounds. Regardless the HDPE source, Nap and Me-Nap have a Type III isotherm, and α -Naphthol presents a Type II isotherm. Nap and Me-Nap fitted to Freundlich isotherm of an unfavorable process ($n = 2.12$ and 1.11 ; 1.87 and 1.31 , respectively), with positive values of ΔH° (50 and 77.17 ; 66 and 64.63 kJ mol^{-1}) and ΔS° (0.070 and 0.0145 ; 0.122 and 0.103 kJ mol^{-1}) for commercial and waste MP, respectively. Besides, the adsorption isotherm of α -Naphthol on commercial and waste HDPE fitted to the Langmuir model ($Q_{\text{max}} = 42.5$ and 27.2 $\mu\text{mol g}^{-1}$, respectively), presenting negative values of ΔH° (-43.71 and -44.10 kJ mol^{-1}) and ΔS° (-0.037 and -0.025 kJ mol^{-1}). The adsorption kinetic study presents a nonlinear pseudo-second-order model for all cases. The K_2 values follow the order Me-Nap $>$ Nap $>$ α -Naphthol in both MP. Therefore, this experimental study provides new insights into the affinity of PAH derivatives for a specific class of MP, helping to understand the environmental fate of residual MP and organic pollutants.

Keywords: HDPE microplastics, adsorption mechanisms, Nap derivatives, functional groups

LIST OF FIGURES

Figure 1: Scanning electron microscopy for (a) commercial HDPE (5000×); (b) commercial HDPE (15000×); (c) waste HDPE (15000×); and (d) waste HDPE (15000×).	29
Figure 2: Raman (a) and FTIR (b) spectra for commercial (blue lines) and waste (red lines) HDPE MP.	30
Figure 3: ESP distributions (a) Naphthalene; (b) Me-Naphthalene; (c) α -Naphthol; (d) α -Naphtholate;	32
Figure 4: Nonlinear isotherms for Nap, Me-Nap and α -Naphthol onto (a) commercial and (b) waste HDPE. Dotted lines represent the Freundlich isotherm fitting and dashed lines represent the Langmuir isotherm fitting.	34
Figure 5: Pseudo-second-order plot. (a) PAH adsorbed onto commercial HDPE; (b) PAH adsorbed onto waste HDPE.	38
Figure 6. S1: Analytical curves for PAH studied.	43
Figure 7. S2: (a) β -Naphthol; (b) β -Naphtholate.	44
Figure 8. S3: Freundlich isotherm linear graph. (a) and (b) Naphthalene (blue balls) onto commercial and waste HDPE; (c) and (d) Me-Nap (orange triangles) onto commercial and waste HDPE; (e) and (f) α -Naphthol (green square) onto commercial and waste HDPE.....	45
Figure 9. S4: Nonlinear Langmuir isotherms. (a) and (B) Nap onto commercial and waste HDPE; (b) and (c) Me-Nap onto commercial and waste HDPE.	46
Figure 10. S5: Spectrum on different pH values. (a) α -Naphthol; (b) β -Naphthol.	46
Figure 11. S6: α -Naphthol and β -Naphthol on pH < 9.4.	47
Figure 12. S7: Dubinin-Radushkevich linear isotherm. (a) and (b) Nap (blue balls) onto commercial and waste HDPE; (c) and (d) Me-Nap (orange triangles) onto commercial and waste HDPE (e) and (f) α -Naphthol (green square) onto commercial and waste HDPE.....	47
Figure 13. S8: Dubinin-Radushkevich nonlinear isotherm. (a) and (b) Nap (blue balls) onto commercial and waste HDPE; (c) and (d) Me-Nap (orange triangles) onto commercial and waste HDPE (e) and (f) α -Naphthol (green square) onto commercial and waste HDPE.....	48
Figure 14. S9: Isotherm at different temperatures. (a) Nap onto HDPEc; (b) Nap onto HDPEw; (c) Me-Nap onto HDPEc; (d) Me-Nap onto HDPEw; (e) α -Naphthol onto HDPEc; (f) α -Naphthol onto HDPEw.	50

Figure 15. S10: Linear plot of $\ln K_c$ versus $1/T$ for the adsorption of PAHs on microplastics at different temperatures.....	51
Figure 16. S11: Pseudo-first order linear graph. (a) PAHs onto commercial HDPE; (b) PAHs onto waste HDPE.	53
Figure 17. S12: Pseudo-first order nonlinear graph. (a) Nap onto commercial HDPE; (b) Nap onto waste HDPE; (c) Me-Nap onto commercial HDPE; (d) Me-Nap onto waste HDPE; (e) α -Naphthol onto commercial HDPE; (f) α -Naphthol onto waste HDPE.	54
Figure 18. S13: Pseudo-second order linear graph. (a) Nap and Me-Nap onto commercial HDPE; (b) Nap and Me-Nap onto waste HDPE. (c) α -Naphthol onto commercial HDPE; (d) α -Naphthol onto waste HDPE.	54
Figure 19. S14: Intraparticle diffusion plot. (a) adsorption of Nap, Me-Nap and α -Naphthol onto commercial HDPE. (b) adsorption of Nap, Me-Nap and α -Naphthol onto waste HDPE.....	55

LIST OF TABLES

Table 1: Physical, chemical and physicochemical parameters, at 25 °C, of the main PAHs listed by the US EPA (Adapted from Finlayson-Pitts and James N. Pitts (2000b)).	14
Table 2: Physical and chemical properties of the 16 PAH listed by the US EPA and their respective TEFs	16
Table 3: relative data to carcinogenic, genotoxic and mutagenic effects os some PAH and its derivatives.....	17
Table 4: Density and Glass transition temperature for some polymers.....	19
Table 5: Nonlinear isotherm parameters	34
Table 6. S1: Naphthalene and naphthalene derivatives physical and chemical properties.	42
Table 7. S2: Linear isotherm parameters.....	43
Table 8. S3: Relationship between isotherm parameters and curve type.	44
Table 9. S4: Thermodynamic parameters for adsorption of Nap and its derivatives onto commercial and waste HDPE.	49
Table 10. S5: Nonlinear kinetic parameters for PAH.....	51
Table 11. S6: Linear kinetic parameters.....	52

TABLE OF CONTENTS

RESUMO.....	5
ABSTRACT	6
LIST OF FIGURES.....	7
LIST OF TABLES.....	9
TABLE OF CONTENTS	10
MOTIVATION AND OBJECTIVES	12
CHAPTER I – Literature Review	13
Polycyclic Aromatic Hydrocarbons	13
Exposure to Polycyclic Aromatic Hydrocarbons.....	15
Effects of long-term exposure to PAH.....	17
Microplastics and interactions with polycyclic aromatic hydrocarbons.....	19
CHAPTER II – Adsorption of naphthalene and its derivatives onto high-density polyethylene microplastic: Computational, isotherm, thermodynamic, and kinetic study.....	21
ABSTRACT	23
2.1 INTRODUCTION	24
2.2 MATERIALS AND METHODS.....	26
2.2.1 Adsorbents and Adsorbates	26
2.2.2 Preparation of working solutions	26
2.2.3 Preparation of waste polyethylene adsorbent	26
2.2.4 Characterization of adsorbents.....	26
2.2.5 Electrostatic surface potential analysis	27
2.2.6 Adsorption assays	27
2.3 RESULTS AND DISCUSSION.....	28
2.3.1 Characterization of adsorbents.....	28
2.3.2 Computational model for the adsorption study.....	30

2.3.3 Adsorption isotherms	32
2.3.4 Adsorption thermodynamics	35
2.3.5 Adsorption kinetics	36
2.4 CONCLUSION	38
Credit authorship contribution statement.....	39
Declaration of competing interest.....	39
Funding	39
2.5 SUPPLEMENTARY INFORMATION	40
CHAPTER III- General Conclusions	56
REFERENCES	58

MOTIVATION AND OBJECTIVES

This work begins with the analysis of the literature on the adsorption of organic compounds in polyethylene plastics, published in journals with a high impact factor in recent decades. With this, it was possible to verify some gaps not yet explored, thus motivating this work. Most of the literature reports the use of commercial polymeric adsorbents and not properly residual adsorbents. In addition, the studies carried out use several aromatic organic pollutants, and very little is explored about their derivatives, such as the presence of different functional groups. Combining these main factors, this work seeks to bring the adsorptive study of naphthalene and its derivatives in commercial and residual adsorbents of high-density polyethylene.

The expected goals for this work

- To investigate the adsorption of naphthalene and naphthalene derivatives with different functional groups onto high-density polyethylene (HDPE) commercial and residual microplastics of HDPE.
- To understand the influence of functional groups on the adsorption of these PAH
- To explore the behavior and feasible interactions between MP and Nap and Nap derivatives, electrostatic surface potential (ESP) analysis was performed.
- To study the behavior of adsorption, isotherm, thermodynamic and kinetic were performed.

CHAPTER I – LITERATURE REVIEW

Polycyclic Aromatic Hydrocarbons

PAH are a class of compounds characterized by having condensed aromatic rings. They constitute an important class of pollutants, leading to significant environmental problems. These substances, as well as their nitrated and oxygenated derivatives, are widely distributed and are found as constituents of complex mixtures in the environment. PAHs originate from the incomplete combustion or pyrolysis of organic materials, being released into the environment, ubiquitously, as complex mixtures (Finlayson-Pitts e James N. Pitts, 2000). These compounds are propagated in numerous places by the emission of different combustion sources, such as automotive fuels (diesel and gasoline), biomass burning, wood burning, and residential heating systems. (Finlayson-Pitts e James N. Pitts, 2000).

PAH have low solubility in water, which is expected due to their non-polar character. Compounds with two rings are slightly more soluble, with solubility decreasing with the increase in number of rings. However, from PAH reactions, more soluble compounds such as nitro-PAH, ketones, quinones, lactones and dicarboxylic acids can be formed. Due to its lipophilic character and wide environmental distribution, the risk of human contamination by these substances, together with their derivatives, is high, which occurs by their absorption through the skin or by ingestion and inhalation, being rapidly distributed throughout the body. The presence of PAH in the atmosphere occurs in the form of gases, solids adsorbed or absorbed on the surface of aerosols and by dispersion between the gaseous and particular phases of semi-volatile compounds with 3 and 4 rings. In Brazil, studies on PAH and/or B[a]P concentrations, have shown concentrations of around 0.28 ng m^{-3} in the urban area of São Paulo (Finlayson-Pitts and James N. Pitts, 2000). **Table 1** presents some physical and chemical properties of 22 PAHs of importance for environmental studies.

Table 1: Physical, chemical and physicochemical parameters, at 25 °C, of the main PAHs listed by the US EPA (Adapted from Finlayson-Pitts and James N. Pitts (2000b)).

PAH	Vapor pressure				Solubility <i>S</i> (mg L ⁻¹)	Log <i>K</i> _{OW}	Constante de Henry (<i>H</i>) (Pa m ³ mol ⁻¹)	log <i>K</i> _{OA}
	<i>p</i>		<i>p_L</i>					
	Pa	Torr	Pa	Torr				
Nap	10,4	7,8 x 10 ⁻²	36,8	2,76 x 10 ⁻¹	31	3,37	43	5,13
1-MeNap	8,84	6,63 x 10 ⁻²	8,8	6,6 x 10 ⁻²	28	3,87	45	5,61
2-MeNap	9	7 x 10 ⁻²	11,2	8,4 x 10 ⁻²	25	3,86	51	–
BP	1,3	9,8 x 10 ⁻³	3,7	2,8 x 10 ⁻²	7	3,90	29	–
Ace	3 x 10 ⁻¹	2 x 10 ⁻³	1,5	1,1 x 10 ⁻³	3,80	4,00	12,17	6,23
Act	9 x 10 ⁻¹	6,8 x 10 ⁻³	4,1	3,1 x 10 ⁻²	16,1	4,00	8,4	–
Flu	9 x 10 ⁻²	7 x 10 ⁻⁴	7,2 x 10 ⁻¹	5,4 x 10 ⁻³	1,90	4,18	7,87	6,68
Phe	2 x 10 ⁻¹	1,5 x 10 ⁻⁴	1,1 x 10 ⁻¹	8 x 10 ⁻⁴	1,10	4,57	3,24	7,45
Ant	1 x 10 ⁻³	8 x 10 ⁻⁶	7,78 x 10 ⁻²	5,84 x 10 ⁻⁴	0,045	4,54	3,96	7,34
Pyr	6 x 10 ⁻⁴	4,5 x 10 ⁻⁶	1,19 x 10 ⁻²	8,93 x 10 ⁻⁵	0,132	5,18	0,62	8,43
Flt	1,23 x 10 ⁻³	9,2 x 10 ⁻⁶	8,72 x 10 ⁻³	6,55 x 10 ⁻⁵	0,26	5,22	1,04	8,60
Chr	5,7 x 10 ⁻⁷	4,3 x 10 ⁻⁶	1,07 x 10 ⁻⁴	8,03 x 10 ⁻⁷	0,002	5,75	0,0122	10,44
Trif	2,3 x 10 ⁻⁶	1,7 x 10 ⁻⁸	1,21 x 10 ⁻⁴	9,1 x 10 ⁻⁷	0,043	5,49	0,012	–
BaA	2,80 x 10 ⁻⁵	2,1 x 10 ⁻⁷	6,06 x 10 ⁻⁴	4,55 x 10 ⁻⁶	0,011	5,91	0,581	10,80
BaP	7,0 x 10 ⁻⁷	5,3 x 10 ⁻⁹	2,13 x 10 ⁻⁵	1,60 x 10 ⁻⁷	0,0038	6,04	0,046	10,71
BeP	7,4 x 10 ⁻⁷	5,6 x 10 ⁻⁹	2,41 x 10 ⁻⁵	1,81 x 10 ⁻⁷	0,004	–	0,020	11,13
Per	1,4 x 10 ⁻⁸	1,1 x 10 ⁻¹⁰	–	–	0,0004	6,25	0,003	11,70
BbF	–	–	–	–	0,0015	5,80	–	–
BkF	5,2 x 10 ⁻⁸	3,9 x 10 ⁻¹⁰	4,12 x 10 ⁻⁶	3,09 x 10 ⁻⁸	0,0008	6,00	0,016	11,19
BghiPe	–	–	2,25 x 10 ⁻⁵	1,69 x 10 ⁻⁷	0,00026	6,50	0,075	–
DBA	3,7 x 10 ⁻¹⁰	2,8 x 10 ⁻¹²	9,2 x 10 ⁻⁸	6,9 x 10 ⁻¹⁰	0,0006	6,75	0,00017	13,91

PAHs and their derivatives are present not only in the atmosphere, but also in street dust, soils and aqueous environments, as well as in living organisms (Yang, Z. Z. et al., 2015). There are studies aimed at understanding the transport and transformation of PAHs in various media, such as atmospheric and aquatic (Manzetti, 2013; Bai et al., 2014; Wei et al., 2015). It has been noticed that the generation of these compounds by anthropogenic activities does not only influence the local region, but also other locations, as they are dispersed throughout the globe, with their deposition occurring in remote regions such as Antarctica and the Amazon rainforest (Vecchiato et al., 2015). In such studies, the authors were able to identify which compounds and to what extent they are carried by the environment, together with the carcinogenic risk of each one, as well as the environmental risk arising from their presence (Yang, W. et al., 2015).

Exposure to Polycyclic Aromatic Hydrocarbons

The first appearance of chemical carcinogenicity from organic combustion products was identified in 1775, when chimney sweeps started getting more cancer diagnoses. Furthermore, years later, this problem was attributed to the presence of B[a]P in the samples. However, it was experimentally shown that the carcinogenic activity was not attributed only to B[a]P, but a set of HPA and its derivatives. The PAHs are known to be persistent organic pollutants (POPs), are contaminants in general environments and their excessive exposure can pose risks to the health of humans and animals, and among the various existing PAHs, only 16 are listed as priority contaminants US EPA (**Table 2**).

Resulting from incomplete processes of combustion and pyrolysis of organic carbons that include coals, oil and biomass, these compounds are present everywhere in the environment, in soil, food, air, sediments and dust. According to USEPA, seven compounds are characterized as probable carcinogens, Benzo[b]fluoranthene, Benzo[k]fluoranthene, Benzo[a]pyrene, Chrysene, [a,h] Anthracene and Indene [1, 2,3cd] Pyren. Of these, there are three main ways of contamination by PAH in humans: inhalation, with smoke (actively or passively), ingestion and dermal contact, which cause an increase in the concentration of such substances in the body (Bansal & Kim, 2015; Beriro et al., 2016; Galarneau, 2008; Menezes et al., 2015; Nielsen et al., 2015; Ruby & Lowney, 2012; Xiang et al., 2018).

Table 2: Physical and chemical properties of the 16 PAH listed by the US EPA and their respective TEFs

HPA	Number of aromatic rings	MW	BP	*Carcinogenicity IARC/US EPA
Naphthalene	2	128,17	217,9	2B
acenaphthylene	2	152,20	-	NC
acenaphthene	2	154,21	279	3
Fluorene	2	166,22	295	3
Anthracene	3	178,23	342	3
Fenantreno	3	178,23	340	3
Fluoranthene	3	202,26	375	3
Pyrene	4	202,26	393	3
Benzo[a]anthracene	4	228,29	400	2B
Chrisene	4	228,29	448	2B
Benzo[b]fluoranthene	4	252,31	-	2B
Benzo[k]fluoranthene	4	252,32	480	2B
Benzo[a]pyrene	5	252,32	496	1
Dibenzo[a,h]anthracene	5	278,35	524	2A
Indeno[1,2,3-d]pyrene	5	276,34	536	2B
Benzo[ghi]perylene	6	276,34	545	3

MW- Molecular Weight . **BP**- Boiling Point. *Carcinogenicity to humans: 1 = carcinogenic to humans and animals; 2A = probable human carcinogen – limited in humans and sufficient in animals; 2B = possible human carcinogen – limited evidence in humans and insufficient evidence in animals; 3 = not classified as carcinogenic in humans; NI = not included.

The exposure to PAH is linked to several health effects including toxicity and carcinogenicity. Effects such as inflammation (Ferguson et al., 2017), infertility, fetal malformation (Sexton et al., 2011), oxidative stress (Wang et al., 2015) and cardiovascular disease (Jomova et al., 2012). Short-term effects of exposure to PAHs tend to manifest in the form of skin irritation, nausea and vomiting, and inflammation (Kim et al., 2013). On the other hand, long-term exposures tend to be more violent and carry greater risks, such as various types of cancer, DNA and RNA protein damage, and gene mutation (Kim et al., 2013; Moorthy et al., 2015).

Effects of long-term exposure to PAH

Table 3, shows data about carcinogenicity, genotoxicity and mutagenicity of some PAH and its derivatives. Reactive metabolites of some PAH have greater health effects due to their potential interaction with cellular DNA and proteins. This type biochemical dysfunction together cell damage leads to mutations, development of malformations, tumors and cancers. Furthermore, PAHs have the potential to interfere with hormonal systems, having unhealthy implications for reproduction and immune function. As such, DNA damage induced by PAH exposure has been demonstrated by several authors. Accordingly, polycyclic aromatic hydrocarbons become carcinogenic following activation by metabolizing enzymes to reactivate biotransformation products, which attack cellular DNA. Thus, this change in the DNA sequence in genes that regulate cell replication may increase the possibility of cancer and other diseases reported in several studies in the literature. The result of the mutagenic biotransformation of PAHs includes substances such as diol, epoxides, quinones and HPA radical cations that coordinate with DNA forming bulky complexes called DNA adducts (Ewa & Danuta, 2017).

Table 3: relative data to carcinogenic, genotoxic and mutagenic effects os some PAH and its derivatives.

PAH	Carcinogenicity	Genotoxicity	Mutagenicity
Fluorene	I	L	–
Phenanthrene	I	L	+
Anthracene	N	N	–
Fluoranthene	N	L	+
Pyrene	N	L	+
Benzofluorenes	I	I	NI
Benzofluoranthenes	S	I	+
Cyclopental(cd)pyrene	L	S	+
Benzo(a)Anthracene	S	S	+
Chrysene	L	L	+
Triphenylene	I	I	+
Benzo(e)Pyrene	I	L	+
Benzo(a)Pyrene	S	S	+
Perylene	I	I	+

Indene(1,2,3-d) Pyrene	S	I	+
Dibenz(ac)Anthracene	L	S	+
Dibenz(a)Anthracene	S	S	+
Dibenz(aj)Anthracene	L	I	+
Benzo(ghi)Perylene	I	I	+
Anthracene	L	I	+
Coronene	I	I	+
Dibenzo(ae)Fluoranthene	L	N	
Dibenzopyrenes	S	I	+
2-nitronphthalene	N	L	-
1-nitropyrene	I	S	+
Dinitropyrene			+

Data available for effect comprovation: S= sufficient; I: insufficient; L: limited; N: non carcinogenic. Genotoxicity was evaluated by DNA deterioration tests; chromosomal aberration, mutagenicity. Mutagenicity (Ame tests): + (positive); - negative; NI= not included.

The exposure of women during the gestational period to PAHs is of special importance, since in this way the fetus is exposed to such compounds. The brain development process during pregnancy is extremely vulnerable and such premature exposure can result in brain damage (Schroeder, 2011). Among the reported effects during pregnancy that negatively affect the fetus are abnormal weight and head circumference, low levels of estradiol and testosterone in umbilical cord serum. The toxicity of PAHs present in the pregnant woman's body has also been related to cases of abortion. Prenatal exposure, or even during the first years of the child's life, is also related to cases of growth failure and the development of behavioral problems, such as attention deficit hyperactivity disorder (ADHD) (Jedrychowski et al., 2015).

These effects in adult men can lead to atrophy in the testicles and a decline in sperm quality, as well as decreased testosterone levels. In the West, colon cancer (part of the large intestine) is very common, influenced mainly by environmental factors, without significant participation of family history or sporadic genetic damage being noticed. Diet is one of the main factors leads to susceptibility to gastrointestinal cancer, mainly due to chemical contaminants present in food. Because they easily accumulate in soil, food contamination by PAH occurs in virtually any culture medium, and their presence in the intestinal tract favors the development of tumors. Ingestion of HPA, by whatever route,

may also influence the modulation of drug transporter proteins, plasma proteins, the action of enzymes responsible for drug metabolism and can also cause liver damage. Thus, exposure to PAH ends up influencing the body's response to medications, interfering in the fight against diseases (Diggs et al., 2011).

Microplastics and interactions with polycyclic aromatic hydrocarbons

Microplastics (MP) are defined as particles of ≤ 5 mm of diameter, having characteristics such as hydrophobicity and large surface area. These materials are commonly used on manufacture and needs basic. The global utilization of plastic increased over decades, and the main polymers types utilized are (PE), polypropylene (PP), polyvinyl chloride (PVC), polystyrene (PS), and polyamide (PA, commonly known as nylon) (Prajapati et al., 2022 and Mei, et al., 2020). Generally, plastics are dispersed in the environment due to large production and irregular disposal. In 2018 the production of plastic registered 359 million of tons (MT) and can double in 20 years (Andrady 2019). In the environment, these tones of plastics are affected by weathering through physical and chemical degradation, generating MP, which are widely distributed in ecosystems, mainly in the marine environment. On the other hand, the MP can act as carriers for organic pollutants present in the aquatic system. However, MP-sorbed organic compounds can cause ecological risks to organisms through MP ingestion. The process where organic compounds are fixed in MP surface is known as adsorption. Furthermore, about 16 PAHs have been reported in the Bohai and Huang Hai Seas, in China, in surface waters, reaching concentrations of 3400—119,000 ng g⁻¹ in MP (Mai et al., 2020). MP have some interactions mechanisms with Persistent Organic Pollutants (POP), such as PCBs and organochlorine pesticides and PAH, for example. Hydrophobic organic contaminants (HOC) interact with MP via hydrophobic interactions, and this interaction can be influenced by some of MP's characteristics, such as polymer type and crystallinity, size and shape, age of plastics, degree of weathering and color (Prajapati et al., 2022; Mei et al., 2020). The main interactions involving MP and PAH are π - π , van der Waals forces, hydrophobic and H-bonding interactions (Liu et al., 2019).

Table 4 shows some polymers and their structure, besides glass transition temperature (T_g). Due to all of these factors, studies involving MP, HOC and PCBs will help in the understanding of the effects that these possess on global environment.

Table 4: Density and Glass transition temperature for some polymers

Polymer type	Structure	T _g (°C)	Density (g cm ⁻³)
High-density polyethylene (HDPE)	-(CH ₂ -CH ₂) _n -	-125	0.94 to 0.97
Polypropylene (atactic)	-[CH ₂ -CH(CH ₃)] _n -	-20 to -5	0.85 to 0.94
Polyamide (Nylon 6,6)	-[CO(CH ₂) ₅ NH] _n -	50 to 60	1.13 to 1.15
Polyvinyl chloride (PVC)	-(CH ₂ -CHCl) _n -	65 to 85	1.16 to 1.20
Polyethylene terephthalate (PET)	(C ₁₀ H ₈ O ₄) _n	70 to 80	1.34 to 1.39
Polyvinyl alcohol	-[CH ₂ CH(OH)] _n -	80 to 90	1.19
Polypropylene (isotactic)	-[CH ₂ -CH(CH ₃)] _n -	100	0.92
Polystyrene (PS)	-[CH ₂ -CH(C ₆ H ₅)] _n -	90 to 110	1.04 to 1.09
Polytetrafluoroethylene (PTFE)	-(CF ₂ -CF ₂) _n -	120 to 130	2.2
Polyurethane (PU)	-RNHCOOR'-	120 to 160	1.2
Polyacrylamide	-[CH ₂ =CH-CONH ₂]-	160 to 170	1.11

Prajapati et al., 2022

CHAPTER II – Adsorption of naphthalene and its derivatives onto high-density polyethylene microplastic: Computational, isotherm, thermodynamic, and kinetic study

Chapter II comprises the article of this dissertation, focused on the adsorption of Naphthalene and its derivatives with functional groups methyl ($-\text{CH}_3$) and hydroxyl ($-\text{OH}$) onto commercial and waste high-density polyethylene (HDPE) microplastics (MP). This work including a detailed computational, isotherm, thermodynamic and kinetic study of mechanisms involving HDPE-PAH interactions and approach the influence of functional groups on adsorption behavior, that little is reported based on literature.

Adsorption of naphthalene and its derivatives onto high-density polyethylene microplastic: computational, isotherm, thermodynamic, and kinetic study

Ronaldo Antunes Funari Junior^a; Lucas Mironuk Frescura^a; Bryan Brummelhaus de Menezes^a; Ana Flávia de Moraes Bastos^a; Marcelo Barcellos da Rosa^{*a}.

^aUniversidade Federal de Santa Maria – UFSM, Department of Chemistry, Av. Roraima, 1000, 97105-900, Santa Maria, RS, Brazil

Corresponding author: Marcelo Barcellos da Rosa e-mail: marcelo.b.rosa@ufsm.br

DOI: 10.1016/j.envpol.2022.120919

Abstract

Microplastics (MP) have received great attention due to the mass-produced residues discharged into the environment. MP are ideal for adhering to organic pollutants that can be easily dispersed, thus posing risks to human health. Furthermore, little has been reported on how different functional groups in polycyclic aromatic hydrocarbons (PAH) derivatives influence the adsorption behavior on MP. To better understand this process, groups methyl ($-\text{CH}_3$) and hydroxyl ($-\text{OH}$) were selected and commercial and waste high-density polyethylene (HDPE, $\leq 1\text{mm}$) were used as adsorbents, and Naphthalene (Nap), 1-Methyl-Naphthalene (Me-Nap) and α -Naphthol as adsorbates. The results showed different behaviors for nonpolar and polar adsorbates. Dispersion forces were the main type of interaction between HDPE and Nap/Me-Nap, while dipole-induced dipole forces and H-bonding were the chief interactions involving MP and polar compounds. Regardless the HDPE source, Nap and Me-Nap have a Type III isotherm, and α -Naphthol presents a Type II isotherm. Nap and Me-Nap fitted to Freundlich isotherm of an unfavorable process ($n = 2.12$ and 1.11 ; 1.87 and 1.31 , respectively), with positive values of ΔH° (50 and 77.17 ; 66 and 64.63 kJ mol^{-1}) and ΔS° (0.070 and 0.0145 ; 0.122 and 0.103 kJ mol^{-1}) for commercial and waste MP, respectively. Besides, the adsorption isotherm of α -Naphthol on commercial and waste HDPE fitted to the Langmuir model ($Q_{\text{max}} = 42.5$ and 27.2 $\mu\text{mol g}^{-1}$, respectively), presenting negative values of ΔH° (-43.71 and -44.10 kJ mol^{-1}) and ΔS° (-0.037 and -0.025 kJ mol^{-1}). The adsorption kinetic study presents a nonlinear pseudo-second-order model for all cases. The K_2 values follow the order Me-Nap > Nap > α -Naphthol in both MP. Therefore, this experimental study provides new insights into the affinity of PAH derivatives for a specific class of MP, helping to understand the environmental fate of residual MP and organic pollutants.

Keywords: HDPE microplastics; Adsorption mechanisms; Nap derivatives; Functional groups

2.1 INTRODUCTION

Large-scale production of polymer in the last decades arises from the increased demand, for its versatility enables it to be used in several products, sectors, and commercial packaging. The increased consumption most often results in irregular polymer waste disposal into riverine systems and, consequently, into seas the oceans. The global annual input of polymer into oceans has been estimated to be between 1.15 and 2.4 million tons (Mei et al., 2020). Polyethylene terephthalate (PET) is the most commonly produced polymer worldwide, followed by high-density polyethylene (HDPE) (Issac and Kandasubramanian, 2021). However, polyethylene-based products like HDPE are the dominant type of waste in aquatic environments (Ekvall et al., 2022; Schwarz et al., 2019). When deposited in the environment, this trash is directly affected by climatic processes, such as physical degradation, thus generating smaller particles, the microplastics (MP), which are characterized by being less than 5mm in size (Andrady, 2017). They accumulate and persist in water, consequently contaminating drinking-water sources and the atmosphere, thus easily entering the human body via the digestive and respiratory systems (Coyle et al., 2020; Horton et al., 2017; Kane and Clare, 2019; Liu et al., 2019; Schwarz et al., 2019; Szewc et al., 2021).

Due to properties like hydrophobicity and surface area, MP have affinity for toxic organic pollutants including herbicides, insecticides, and mainly polycyclic aromatic hydrocarbons (PAH). These substances accumulate on the surface of MP by adsorption and disperse in the environment (Liu et al., 2019; Yu et al., 2020). When ingested or inhaled by humans, such compounds may desorb in the organism and generate health problems such as hormonal, immunological, neurological, and reproductive dysfunctions (Liu et al., 2019; Saad et al., 2019).

PAH have two or more condensed aromatic rings, are chemically stable, and potentially carcinogenic, teratogenic, and mutagenic to humans (Ewa and Danuta, 2017; Jomova et al., 2012; Kim et al., 2008; Moorthy et al., 2015; Sexton et al., 2011; Wang et al., 2015). The MP serve as a means for these compounds to migrate from one environment to another when inhaled or ingested by living organisms, including humans. The presence of polyethylene particles in human lung tissue has been reported (Amato-Lourenço et al., 2021). Sørensen et al. (2020) mentioned that MP-sorbed organic compounds are an alternative route of exposure to such chemicals in the marine environment. For example, Mai et al. (2018) reported the presence of 16 PAH in MP

collected from seawater in Bohai and Hunghai, China. Usually, adsorption of PAH onto MP occurs due to the hydrophobicity (octanol-water coefficient, K_{ow}) of PAH and characteristics of MP as type, surface area and structure (Jiang et al., 2022).

PAH molecules are ubiquitously found in the environment (Mai et al., 2018), and their main source is combustion of fossil fuels. Naphthalene (Nap) derivatives with functional groups are relatively widespread (Lin et al., 2009). Nap derivatives with methyl ($-CH_3$) and hydroxyl ($-OH$) functional groups are the most emitted PAH, mainly from mobile sources as gas- and diesel-powered vehicles (Lin et al., 2009). Nap and 1-Methyl-Naphthalene (Me-Nap) have been detected in the atmosphere of Los Angeles city at concentrations of about $2.5\mu\text{g m}^{-3}$, and in surface waters particularly after irregular or accidental oil spills (Bytingsvik et al., 2020; Wang et al., 2007). Owing to their greater potential for interaction with human DNA, Nap derivatives such as α and β -Naphthol are even more toxic than the precursor molecule (Ding et al., 2021; Qin et al., 2020).

PAH adsorption studies have been performed with some types of MP to understand the mechanism and behavior related to this process; nevertheless, such evaluations consider simple PAH structures, solely composed of carbon and hydrogen (Wang et al., 2019; Zhao et al., 2020). There is still a lack of information concerning the effect that the presence of functional groups may have on PAH adsorption onto MP, especially HDPE. In this study, batch adsorption experiments were conducted to assess the effects on the isotherms, thermodynamics, and kinetics of adsorption of Nap and its derivatives (Table S1) onto waste HDPE versus commercial HDPE. In addition, electrostatic surface potential (ESP) analysis was carried out to explore this behavior and the feasible interactions between MP and Nap as well as its derivatives.

2.2 MATERIALS AND METHODS

2.2.1 Adsorbents and Adsorbates

Nap (99%, cas n° 91-20-3) and Me-Nap (95%, cas n° 90-12-0) were obtained from Sigma Aldrich® (St. Louis/USA), and α -Naphthol (99%, cas n° 90-15-3) and β -Naphthol (98%, cas n° 135-19-3) were acquired from Dinâmica®. Commercial HDPE (180 μ m) was purchased from Sigma Aldrich® (St. Louis/USA) and waste HDPE was sourced from domestic packaging.

2.2.2 Preparation of working solutions

The stock solutions of Nap, Me-Nap, α -Naphthol and β -Naphthol were prepared in ultrapure water at 150 μ mol L⁻¹ (pH=6.5) and placed in ultrasonic bath for 80 min to ensure complete solubility of the molecules. The analytical curves are shown in Fig. S1. The spectra of the molecules were obtained for UV-vis using a spectrophotometer system Perkin Elmer Lambda 16 double beam with a 10 mm quartz cell according to the specific wavelengths of Nap, Me-Nap, α -Naphthol and β -Naphthol: 277, 283, 334 and 283 nm, respectively. The pH study was made adding 1 ml of HCl solution (0.1M, pH=2) and a buffer solution (pH=11.04) in α -Naphthol and β -Naphthol solutions.

2.2.3 Preparation of waste polyethylene adsorbent

HDPE containers for cleaning chemical products were used to prepare waste HDPE. The packages were subjected to milling in a Knife Mill (Brand Kie, Louveira, Brazil). The material was then passed through a sieve to standardize the diameter of the particles (1 mm) used in the adsorption process. Subsequently, it was washed with methanol HPLC/UV grade (99%, Sigma Aldrich®, St. Louis/USA), filtered, dried in 45°C, and stored in glass vials.

2.2.4 Characterization of adsorbents

The adsorbents were characterized to determine the surface area via the Brunnauer-Emmett-Teller (BET) method. Morphological characterization was performed by scanning electron microscopy (SEM) (Tescan, VEGA-3G, Czech Republic) coupled with a secondary electron detector (SE) for imaging. The samples were coated with gold (sputtering metallization process, using a current of 30 mA for 120 seconds - Desk V

from Denton Vacuum) to carry out the analyses. Fourier transform infrared spectrometry (FTIR) was performed using a Bruker VERTEX 70 spectrometer equipped with diamond crystal ATR accessory, in the spectral window from 4000 to 400 cm^{-1} . Raman spectroscopy analyses were conducted on a Bruker Senterra confocal Raman microscope using the 785 nm laser in the region of 3500-50 cm^{-1} .

2.2.5 Electrostatic surface potential analysis

Electrostatic surface potential (ESP) analysis was conducted to show the molecular polarity of Nap and its derivatives. The molecular structures of Nap and its derivatives were first drawn in GaussView 6.0 and optimized by Gaussian 09W using the DFT model at the B3LYP/6-311G** basis set. After selecting the correspondent parameters, data on the molecular dipole moments were rapidly given by software in database file format.

2.2.6 Adsorption assays

Adsorption isotherm experiments were performed in triplicate at room temperature ($25 \pm 1^\circ\text{C}$) for 24h under constant stirring on an orbital shaker (200 rpm), with 0.5 g of commercial and waste HDPE MP and 100 mL of the individual solutions of Nap, Me-Nap, α -Naphthol and β -Naphthol at a concentration range of 40 to 150 $\mu\text{mol L}^{-1}$ (Eq. S2-S9) (Chen et al., 2022). Thermodynamic experiments were conducted from the adsorption isotherms at four temperatures (283.15, 298.15, 308.15 and 318.15 K) and calculated by Eq. S10-S14 (González-López et al., 2022). The kinetic adsorption experiments used Nap, Me-Nap and α -Naphthol at an initial concentration of 150 $\mu\text{mol L}^{-1}$, which was placed under constant stirring on an orbital shaker (200 rpm); 3 mL aliquots were collected at the indicated time intervals for 300 min. The measurements were performed using a Perkin Elmer Lambda 16 spectrophotometer system operated in double beam mode with a 10 mm quartz cell. The adsorption tests were evaluated for spectrum signal decay in the defined wavelength, and the amount of removed PAH (qe) was calculated by Eq. S1. Nonlinear fitting was performed with the Solver package in Microsoft Excel, employing the Root Mean Square Error (RMSE) as the parameter to be minimized (Tran et al., 2017).

2.3 RESULTS AND DISCUSSION

2.3.1 Characterization of adsorbents

The morphology of commercial and waste HDPE MP is shown by SEM images (Fig. 1). The rougher surface and greater porosity of commercial HDPE compared with waste HDPE were also confirmed by a higher BET analysis for specific surface area, pore volume and pore size of commercial HDPE comparing with waste HDPE. A more porous surface may be seen at 5000-15000X (Fig. 1a-d). At the same magnification, the presence of roughness may be observed in different regions of the waste HDPE (Fig. 1c-d). Similar morphologies had been previously reported (Li et al., 2021; Wang et al., 2021). The BET analysis indicated that commercial HDPE has a total BET surface area of $2.8191 \text{ m}^2 \text{ g}^{-1}$, and pore volume and pore size of $0.020450 \text{ cm}^3 \text{ g}^{-1}$ and 290.1561 \AA , respectively. Waste HDPE presented BET surface area and pore volume very near the detection limit of the equipment, and the pore size was too small: $0.1749 \text{ m}^2 \text{ g}^{-1}$, $0.000057 \text{ cm}^3 \text{ g}^{-1}$ and 13.0910 \AA , respectively. Although the hydrophobicity of HDPE was not characterized, the measured characteristics and general properties of this polymeric material reveal indirect information; for example, it is highly hydrophobic based on its fully linear molecular structure, favoring interactions with hydrophobic organic compounds (Zhao et al., 2020). The crystalline structure of MP is also an important factor for the adsorption of hydrophobic organic contaminants (HOC). HDPE has a degree of crystallinity of about 80-90%, and is classified as a polymer with rubbery subfraction characteristics (Mei et al., 2020). Recent studies indicate that MP with predominantly crystalline regions adsorb more HOC at low concentrations; moreover, MP with characteristics of rubber components show a higher adsorptive capacity due to the abundant free volume between the molecular chains (Velez et al., 2018; Wang et al., 2019b; Zuo et al., 2019).

The FTIR spectra of both commercial and waste HDPE basically show the same peaks (Fig. 2b), being symmetric and asymmetric CH_2 stretching (2915 cm^{-1} and 2848 cm^{-1} , respectively), CH_2 bending at 1471 cm^{-1} , and split CH_2 rocking vibrations (730 cm^{-1} and 717 cm^{-1}) (Dilshad et al., 2022; Karlsson et al., 2020). The infrared peaks are characteristic of HDPE, differing from low-density polyethylene (LDPE) in the proportion of 1471 cm^{-1} peak and a very small peak in 1369 cm^{-1} (CH_3 umbrella bending), indicating a small amount of terminal methyl groups (Karlsson et al., 2020). The splitting in the CH_2 rocking vibrations (in-plane and out-of-plane) indicates regions of crystallinity in the HDPE (Smith, 2018). Raman analysis shows relevant peaks mainly

in the $1500\text{-}1000\text{ cm}^{-1}$ region (Fig. 2a). The anti-symmetric (1062 cm^{-1}) and symmetric (1129 cm^{-1}) C–C stretching modes of the skeletal chains and the broad weak peak around 1080 cm^{-1} assigned to the C–C stretching mode of the amorphous chains are characteristic of HDPE (Strobl and Hagedorn, 1978). The strong band observed at 1295 cm^{-1} is assigned to the CH₂ twisting modes of the crystalline chains (Sato et al., 2002). A weak CH₃ wagging peak appears at 1369 cm^{-1} (Furukawa et al., 2006). Three distinctive peaks around 1400 cm^{-1} are assigned to the CH₂ bending modes. The narrow doublets situated at 1416 and 1440 cm^{-1} are assigned to the CH₂ bending in the orthorhombic crystal; the band located at 1462 cm^{-1} is assigned to the CH₂ bending modes of the melt-like amorphous chains (Furukawa et al., 2006; Strobl and Hagedorn, 1978).

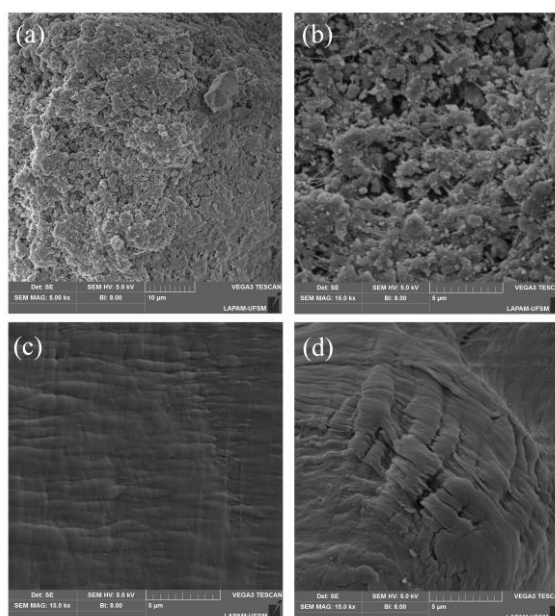


Figure 1: Scanning electron microscopy for (a) commercial HDPE (5000 \times); (b) commercial HDPE (15000 \times); (c) waste HDPE (15000 \times); and (d) waste HDPE (15000 \times).

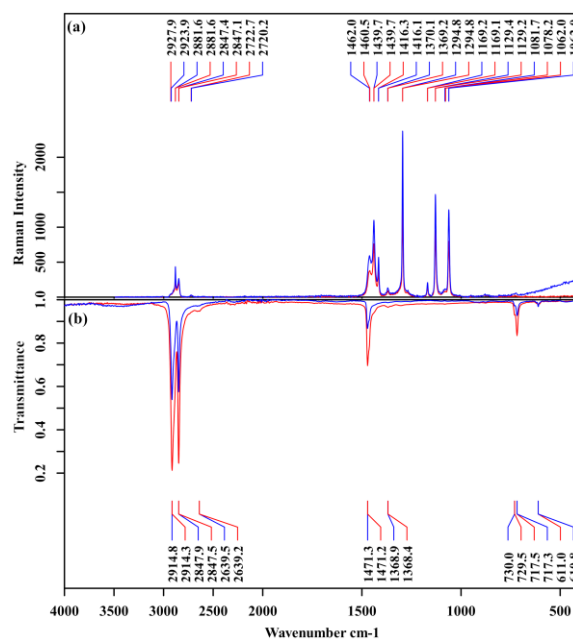


Figure 2: Raman (a) and FTIR (b) spectra for commercial (blue lines) and waste (red lines) HDPE MP.

2.3.2 Computational model for the adsorption study

The ESP can reflect the density of balanced and unbalanced charge distribution on a molecular surface (Lu and Chen, 2012). The surface charge can indicate the feasible interactions between adsorbate and adsorbent: hydrophobic effect, van der Waals force, hydrogen bonding and π - π stacking (Prajapati et al., 2022). In Nap and Me-Nap (Fig. 3a-b), areas with negative potential may be observed inside the molecules (in red) due to the greater electronegativity of the aromatic rings compared with the hydrogens; there are also areas with positive potential distributed outside the molecules (in blue). In comparison, Nap and its derivatives with functional groups induced some negative or positive charges in the molecules (Fig. 3b-f).

Nap and its derivative with uncharged functional group (Me-Nap) demonstrated a better adsorption capacity than the derivatives with charged functional groups (α -Naphthol and β -Naphthol), whose adsorption onto HDPE MP is inhibited due to decreased hydrophobicity and increased solubility (Yu et al., 2020). In addition, as regards adsorption of micropollutants onto activated carbon, properties such as LogK_{ow} showed a better correlation for hydrophobic than hydrophilic compounds (Nam et al., 2014). Therefore, hydrophobicity also plays a decisive role in the adsorption process of PAH on MP. Recent investigations disclose that this property is directly linked to the adsorption of pollutants on MP (Kinigopoulou et al., 2022; Luo et al., 2022; Mateos-Cárdenas et al., 2021). It is directly indicated by the values of LogK_{ow} , which were higher

for Nap and Me-Nap than for α -Naphthol and β -Naphthol (Table S1). Substances showing high values of $\text{Log}K_{ow}$ adsorb more hydrophobic compounds that have a weak interaction with water, such as PAH with two or more aromatic rings (Hüffer and Hofmann, 2016; Wang et al., 2018; Yu et al., 2020).

The dipole moment (μ) may also be used to explain this behavior. The μ values for Nap, Me-Nap, α -Naphthol, deprotonated α -Naphthol, β -Naphthol and deprotonated β -Naphthol were calculated by GaussView: 0.0004D, 0.38D, 1.72D, 5.66D, 1.84D and 7.47D, respectively. The charge of the functional groups causes a variation in the polarity of PAH. High μ values indicate more polar molecules, which means that these molecules form hydrogen bonds with water; this affinity is so strong that it is difficult for the adsorbate to migrate from the solution to the surface. This may explain why the amounts of adsorbed (q_t) Nap and Me-Nap are greater than those of α -Naphthol (Fig. 5). The fast rates of Nap and Me-Nap adsorption may be attributed to the absence of charged functional groups and low molecular polarity (Kronberg, 2016; Mei et al., 2020; Nam et al., 2014; Prajapati et al., 2022). As shown in Fig. 3a-b, Nap and Me-Nap have a negative charge density in benzene rings, implying that they bind to MP through hydrophobic interactions, which is the main mechanism of adsorption involving HDPE. π - π stacking may also occur; nevertheless, this is a weak form of interaction (Hüffer and Hofmann, 2016; Prajapati et al., 2022). The van der Waals force is predominant in the deprotonated α -Naphthol (Fig. 3e), which is a less hydrophobic compound. Nonetheless, the potentially negative surface charge of the molecule can interact with HDPE by hydrogen bonding. van der Waals and H-bonding forces are weaker than π - π and hydrophobic interactions, thus explaining the results obtained for Nap and Me-Nap, in which the hydrophobic effect predominates (Prajapati et al., 2022; Torres et al., 2021).

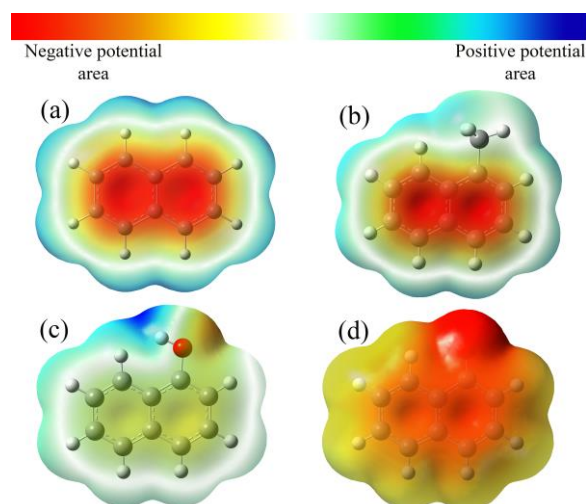


Figure 3: ESP distributions (a) Naphthalene; (b) Me-Naphthalene; (c) α -Naphthol; (d) α -Naphtholate;

2.3.3 Adsorption isotherms

The adsorption isotherms allow a better understanding of the adsorption mechanisms. Different isotherm models (Eq. S2-S9) were tested in order to verify the maximum adsorption capacity of PAH onto commercial and waste HDPE. The shape of the equilibrium curve helps explaining certain phenomena associated with the adsorbate-adsorbent interaction. The findings indicate that adsorption of Nap and Me-Nap on commercial and waste HDPE results in Type III isotherms, described by the Freundlich isotherm (Table 5), based on linear fitting (Table S2 and Fig. S3) and nonlinear curves (Fig. 4a-b). Adsorption is unfavorable when $n > 1$ in the Freundlich isotherm, which is convex shaped curve (sigmoidal isotherm). Therefore, monolayer formation cannot be identifiable, the adsorbent-adsorbate interactions are relatively weak, and the adsorbed molecules are clustered around the most favorable sites on the surface of a nonporous or macroporous solid (Thommes et al., 2015). Thus, no significant adsorption takes place at low concentrations (Franco et al., 2014; Nassar et al., 2014). Such classification is in accordance with Wang et al. (2019), who revealed unfavorable isotherms in the process of Nap adsorption onto some mesopolymers and microplastics. The Langmuir plots for Nap and Me-Nap presented $R_L=1$, calculated from Eq. S4. A linear isotherm shape was demonstrated, thus not being able to show a maximum adsorption capacity of these PAH. This indicates that the amount adsorbed is proportional to the concentration of PAH (Fig. S4). The shape and curvature of the isotherms can be related with the Freundlich exponent (n) and the separation factor (R_L) (Table S3).

The α -Naphthol and β -Naphthol molecules are very sensitive to pH variation, undergoing a wavelength shift of about 40 and 8 nm, respectively (Fig. S5) (Rahim et al., 2016). The adsorption isotherms of α -Naphthol have a good increase in pH > 9.5; however, they are nearly invariable at lower pH values (Fig. S6). No significant changes in concentration values were seen for β -Naphthol adsorption onto HDPE; therefore, there was no effective adsorption with pH variation, and it was not possible to calculate the isotherm parameters. The improvement in α -Naphthol adsorption at pH > 9.5 was due to the pKa of 9.4; thus, above this pH value, there is a purely deprotonated species in the form of α -Naphtholate (Fig. 3d) that favors adsorption on HDPE by hydrogen bonds and van der Waals interactions. The different behavior of β -Naphthol and β -Naphtholate (Fig. S2) results from the greater interaction of the molecules with the water used as solvent via hydrogen bonds. The position of the O⁻ group attached to the second carbon of the aromatic ring (β -Naphtholate) is less hindered than that of the group attached to the first carbon (α -Naphtholate), as it suffers little influence from the adjacent aromatic ring. This explains the greater μ value of β -Naphtholate and, consequently, the higher solubility in water. As it was not possible to determine the adsorption parameters of β -Naphthol, this molecule will not be dealt with hereafter. The charged derivative compound, α -Naphthol adsorbed onto HDPE presents Type II isotherms, characteristic of the physisorption on nonporous or macroporous adsorbents, described by the Langmuir isotherm. The unrestricted monolayer-multilayer adsorption at high concentrations gives a convex curve, while Point B in the concave part usually corresponds to the completion of a monolayer. $R_L < 1$ showed that the adsorption process was favorable and occurred normally; nevertheless, the Q_{max} value was low in experiments with waste HDPE (Table 1).

Table 5: Nonlinear isotherm parameters

Adsorbate	Adsorbent HDPE	Langmuir			Freundlich			Dubnin-Radushkevich		
		K_L (L μmol^{-1})	Q_{max} ($\mu\text{mol g}^{-1}$)	RMSE	K_F ($\mu\text{mol g}^{-1} \mu\text{mol L}^{-1}$)	n	RMSE	q_{DR} ($\text{kJ } \mu\text{mol}^{-1}$)	E ($\text{kJ } \mu\text{mol}^{-1}$)	RMSE
Nap	Commercial	2.99×10^{-5}	undetermined	10.8	6.25×10^{-3}	2.12	1.72	119	28.4	5.59
	Waste	1.11×10^{-4}	undetermined	3.98	1.64×10^{-2}	1.87	1.67	42.7	47.3	3.12
Me-Nap	Commercial	7.01×10^{-5}	undetermined	2.81	0.782	1.11	1.60	82.0	73.8	8.15
	Waste	1.26×10^{-4}	undetermined	2.74	0.235	1.31	1.65	42.1	75.6	1.74
α -Naphthol	Commercial	1.13×10^{-2}	42.6	0.592	0.821	0.752	0.562	26.2	54.2	17.3
	Waste	1.83×10^{-2}	27.2	0.657	1.04	0.634	0.531	14.4	108	1.13

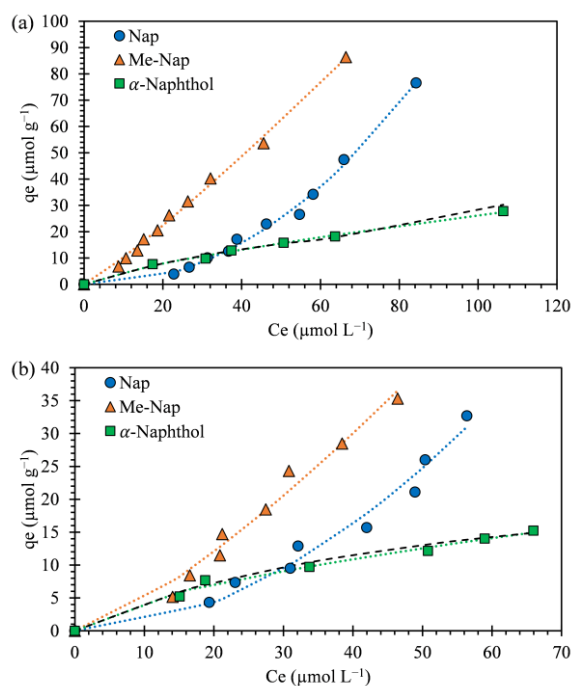


Figure 4: Nonlinear isotherms for Nap, Me-Nap and α -Naphthol onto (a) commercial and (b) waste HDPE. Dotted lines represent the Freundlich isotherm fitting and dashed lines represent the Langmuir isotherm fitting.

The Dubinin-Radushkevich (D-R) isotherm was tested and the results were poor in comparison with those found with the other models applied; the experimental points did not fit into the D-R isotherm model (Fig. S8). The D-R isotherm explains the effect of the porous structure of an adsorbent (Tran et al., 2017) and, as presented in section of Characterization of adsorbents, BET and SEM analyses reveal that the presence of pore is almost negligible, and the surface of the adsorbents is practically smooth. Therefore,

this isotherm is not suitable to explain the adsorption behavior of PAH on commercial and waste HDPE.

2.3.4 Adsorption thermodynamics

The thermodynamics study provides information about the nature of the adsorption process with temperature changes through thermodynamic parameters as ΔG° , ΔH° and ΔS° calculated by (Eq. S10-S14). These parameters were calculated from the adsorption isotherms of Nap, Me-Nap and α -Naphthol on commercial and waste HDPE at four temperatures: 283.15, 298.15, 308.15 and 318.15K. Values of K_C were obtained by Equations S13 and S14 for Nap, Me-Nap and α -Naphthol. The slope and intercept of the plot of $\ln K$ versus $1/T$ (Figure S10) are $-\Delta H^\circ/R$ and $\Delta S^\circ/R$, respectively.

Table S4 shows the thermodynamic parameters for adsorption of Nap and its derivatives. The ΔG° values obtained for Nap and Me-Nap adsorption onto commercial and waste HDPE at four temperatures are positive, indicating that the process was weakly favored as the temperature increased and that it was nonspontaneous (Lim and Kim, 2017). The ΔH° values of adsorption onto commercial and waste HDPE are, respectively: 50.06 and 77.17 kJ mol⁻¹ for Nap, and 66.07 and 64.63 kJ mol⁻¹ for Me-Nap; the ΔS° values are, respectively: 0.070 and 0.145 kJ mol⁻¹ for Nap, and 0.122 and 0.103 kJ mol⁻¹ for Me-Nap. This agrees with what is stated in section of Adsorption isotherms: the isotherms were unfavorable for adsorption onto both HDPE. It demonstrates weak adsorbent-adsorbate interactions, and the findings obtained for ΔG° and ΔH° indicate a nonspontaneous endothermic adsorption process. The endothermic characteristic can be described by considering that the molecules of Nap and Me-Nap lose part of their hydration layer when adsorbed. This process consumes energy, which exceeds the energy released when PAH binds to the adsorbent surface (Anastopoulos and Kyzas, 2016; Yang et al., 2010). Moreover, the positive ΔS° value indicates that the total degree of freedom in the system increases with PAH adsorption. This is in keeping with the results found by Saleh et al. (2022), who disclosed positive enthalpy and entropy values when assessing the adsorption of Nap and fluorene on polymer modified carbon. Differently, Long et al. (2009) observed a high-exothermic adsorption enthalpy for Nap adsorption onto microporous and hypercrosslinked polymeric adsorbent. When hydrophobic molecules are dissolved in water, the H₂O molecules tend to create cages or cavities around the hydrophobic solute (Fisicaro et al., 2004). This process creates numerous H₂O–H₂O

interactions to energetically compensate the lack of solute–H₂O interactions. However, a high organization of several water molecules is required, thus reducing the total entropy of the system (Fiscaro et al., 2004; Kronberg, 2016), i.e., the solubilization of hydrophobic molecules in water tends to reduce the entropy.

In contrast, the ΔG° values for α -Naphthol adsorption onto commercial and waste HDPE are negative and decrease as the temperature rises, thus indicating a spontaneous process. This is in line with the statement given in section of Adsorption isotherms: $R_L < 1$ results in favorable adsorption. Nonetheless, the process is least favored at a higher temperature. The negative ΔH° values obtained for α -Naphthol adsorption onto commercial and waste HDPE, -43.71 and -44.10 kJ mol⁻¹, respectively, suggest an exothermic adsorption process; the ΔS° values are also negative, -0.037 and -0.025 kJ mol⁻¹, respectively, thus implying a low degree of freedom (Lim and Kim, 2017). This is consistent with what has been found by Zhao et al. (2011) when studying α -Naphthol adsorption on sulfonated graphene nanosheets, indicating a spontaneous and endothermic process.

In general, entropy seems to be the determinant factor in the temperature dependence of the adsorption process of the hydrophobic (Nap and Me-Nap) and hydrophilic (α -Naphthol) PAH. Adsorption of hydrophobic PAH is endothermic, but the entropy is positive, since the organized water cavities are undone (Alaee et al., 1996). The process of α -Naphthol adsorption is exactly the opposite: negative ΔH° and ΔS° entropy. Therefore, temperature dependence of the term $-T \times \Delta S^\circ$ makes the entropy signal determinant for the adsorption K_C to be directly or inversely proportional to temperature (Syamala and Würthner, 2020).

2.3.5 Adsorption kinetics

Fig. 5 demonstrate the PSO adsorption kinetics of Nap, Me-Nap and α -Naphthol on commercial and waste HDPE. In this study, three kinetic models were applied to analyze the experimental data: pseudo-first-order (PFO), pseudo-second-order (PSO) and intraparticle diffusion (ID) (Eq. S15-19). The kinetics of PFO and PSO were selected because they are widely used in processes of adsorption of solute from a liquid solution, being based on the adsorption capacity of the solid (Hu et al., 2022). The results indicate that Nap and its derivatives present distinct equilibrium times due to the presence of different functional groups.

The experimental data ($q_{e \text{ exp}}$) efficiently fitted to the PSO kinetic model; the findings were all based on the nonlinear model calculated from Eq. S17, showing ($q_{e \text{ exp}}$) values very close to the nonlinear PSO fit (Fig. 5). The linear kinetic parameters were also calculated (Table S6), and the R^2 values are given as supplementary information. Therefore, the nonlinear PSO model is more appropriate for calculating the kinetic, presenting insignificant systematic error (Bullen et al., 2021; Tran et al., 2017). Table S5 shows the nonlinear kinetic parameters; the amount adsorbed in equilibrium (q_e) and the nonlinear K_2 values follow the order Me-Nap > Nap > α -Naphthol. Furthermore, according to the scientific literature, the PSO model better describes the adsorption mechanism of two-ring PAH, and generally describes most adsorption kinetic experimental data adequately (Long et al., 2009; Meng et al., 2016; Yu et al., 2020). The PFO model did not describe the experimental data for adsorption of Nap and its derivatives on both HDPE, seen by the experimental data not being close to the PFO fit in accordance with the nonlinear PFO plot (Fig. S11-12). The unknown parameters (q_e and K_1) constitute a problem as regards the application of the linear PFO equation, which is only appropriate for the first 30 min (Tran et al., 2017).

In the ID model, the adsorbate diffuses into the pores of the adsorbent. In a solid-liquid sorption process, adsorbate transfer is often characterized by film diffusion (also known as external diffusion), surface diffusion and pore diffusion, or combined surface and pore diffusion. In summary, adsorption is governed by ID if a plot of qt versus $t^{1/2}$ is linearly fitted and passes through the origin (Fu et al., 2021). The results obtained for the kinetics of Nap and Me-Nap were poorly described by the ID model (Table S5 and Fig. S13). The values of R^2 were low, between 0.5-0.8, if compared with those of the linear PSO (0.999) (Fig. S13). Comparing to Nap and Me-Nap, α -Naphthol showed relatively high R^2 for adsorption onto commercial and waste HDPE: 0.9811 and 0.9787, respectively.

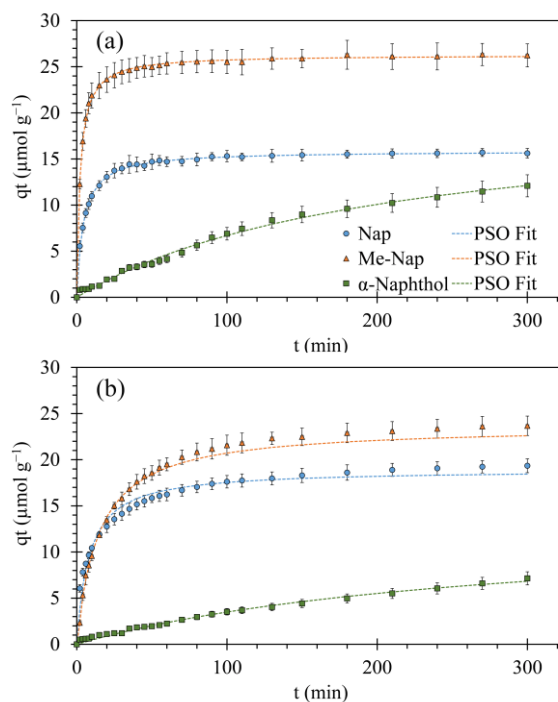


Figure 5: Pseudo-second-order plot. (a) PAH adsorbed onto commercial HDPE; (b) PAH adsorbed onto waste HDPE.

2.4 CONCLUSION

This computational, isothermal, thermodynamic, and kinetic study evaluated the influence of different functional groups ($-\text{CH}_3$ and $-\text{OH}$) on the adsorption behavior of Nap and its derivatives onto commercial and waste HDPE MP in an aqueous system. The findings indicate a lower adsorption capacity of Nap and its derivative with polar functional group (e.g., $-\text{OH}$) compared with the derivative with nonpolar functional group (e.g., $-\text{CH}_3$). Factors as hydrophobicity ($\text{Log}K_{ow}$) have a key role in the adsorption of Nap and its derivatives onto HDPE. The hydroxyl group in α -Naphthol provides higher molecular polarity, which decreases its hydrophobicity and culminates in lower adsorption capacity. The distinct behavior of β -Naphthol results from its greater interaction with water, thereby hampering the determination of the adsorption parameters within the sensibility of the techniques available to conduct this work. The ESP analysis helped to understand the interactions of these PAH with the HDPE surface, which mainly involve hydrophobic, π - π , van der Waals and hydrogen-bonding interactions due to the presence (red regions) or absence (blue regions) of charge on the surface of the molecules (DFT analysis). The adsorption isotherms were unfavorable for Nap and Me-Nap when $n > 1$, with weak adsorbent-adsorbate interactions and an endothermic nature; Q_{max}

value was undetermined. Nevertheless, the observed adsorption occurred due to entropic effects and was slightly enhanced with the increase in temperature. For α -Naphthol, the adsorption isotherm was favorable and best fit to the Langmuir model, indicating an exothermic process. Low temperatures favor adsorption of nonpolar PAH onto HDPE MP. Polar ($-\text{OH}$) functional groups make PAH adsorption favorable under increasing temperatures. Adsorption of Nap and its derivatives onto waste and commercial HDPE conforms to the PSO kinetics, and the nonpolar ($-\text{CH}_3$) functional group has a higher kinetic constant value compared with Nap and α -Naphthol. Knowledge on the adsorption mechanisms of PAH derivatives onto MP is essential to understand the risks associated with this type of interaction; depending on the toxicity of the materials, a higher priority should be given. These findings suggest that HDPE MP may accumulate and carry PAH in the aquatic environment, thus representing multiple risks for environmental and human health; therefore, due caution is required.

Credit authorship contribution statement

Ronaldo Antunes Funari Junior: Conceptualization, Methodology, Development, Investigation, Formal analysis, Writing, Review and Editing. Lucas Mironuk Frescura: Conceptualization, Writing, Review, and editing. Bryan Brummelhaus de Menezes: Conceptualization, Writing – original draft, Review, and editing. Ana Flávia M. Bastos: Methodology, Development, Investigation. Marcelo Barcellos da Rosa: Supervision, Resources, and writing — review and editing.

Declaration of competing interest

The authors declare that they have no known competing financial interests or personal relationships that could have appeared to influence the work reported in this paper.

Funding

This study was financed in part by the Coordenação de Aperfeiçoamento de Pessoal de Nível Superior — Brasil (CAPES) — Finance Code 001 and by Fundação de Amparo à pesquisa do Estado do RS (FAPERGS).

2.5 Supplementary Information

Adsorption isotherms

$$q_e = \frac{(C_0 - C_f)}{m} V \quad (\text{Eq. S1})$$

where q_e is the adsorption capacity in equilibrium ($\mu\text{mol g}^{-1}$), C_0 and C_f are the initial and final concentrations of PAH ($\mu\text{mol L}^{-1}$), respectively, V is the volume of solution (L), and m is the mass of HDPE (g).

Langmuir equation

The Langmuir isotherm can be described for nonlinear and linear forms in Equations S2 and S3:

$$q_e = \frac{Q_{max}^0 K_L C_e}{1 + K_L C_e} \quad (\text{Eq. S2})$$

$$\frac{C_e}{q_e} = \left(\frac{1}{Q_{max}^0} \right) C_e + \frac{1}{Q_{max}^0 K_L} \quad (\text{Eq. S3})$$

where Q_{max}^0 ($\mu\text{mol L}^{-1}$) is the maximum amount of adsorption in adsorbent saturated monolayer, C_e ($\mu\text{mol L}^{-1}$) is the concentration of adsorbate in equilibrium, q_e ($\mu\text{mol g}^{-1}$) is the amount of PAH removed in equilibrium, and K_L ($\text{L } \mu\text{mol}^{-1}$) is a constant of adsorbent and adsorbate affinity.

The essential characteristics of the Langmuir isotherm model can be expressed in terms of a dimensionless constant, the separation factor or equilibrium parameter (R_L), which is defined by Equation S4:

$$R_L = \frac{1}{1 + K_L C_e} \quad (\text{Eq. S4})$$

Freundlich equation

The nonlinear and linear forms of the Freundlich isotherm can be described by Equations 5 and 6:

$$q_e = K_F C_e^n \quad (\text{Eq. S5})$$

$$\log q_e = n \log C_e + \log k_F \quad (\text{Eq. S6})$$

where q_e ($\mu\text{mol g}^{-1}$) is the amount of PAH removed in equilibrium, C_e ($\mu\text{mol L}^{-1}$) is the concentration of PAH in equilibrium, K_F ($\mu\text{mol g}^{-1}/(\mu\text{mol L}^{-1})^n$) is the Freundlich constant, and n (dimensionless) is the Freundlich intensity parameter.

Dubinin-Radushkevich equation

The nonlinear and linear forms of the Dubinin-Radushkevich isotherm can be illustrated as Equations 7, 8 and 9:

$$q_e = q_{DR} e^{-k_{RD} \varepsilon^2} \quad (\text{Eq. S7})$$

$$\ln q_e = -k_{DR} \varepsilon^2 + \ln q_{DR} \quad (\text{Eq. S8})$$

$$\varepsilon = RT \ln \left(1 + \frac{1}{c_e} \right) \quad (\text{Eq. S9})$$

where q_{DR} ($\mu\text{mol g}^{-1}$) is the adsorption capacity, k_{RD} ($\mu\text{mol}^2/\text{kJ}^2$) is a constant related to the sorption energy, and ε is the Polanyi potential.

Adsorption thermodynamics

The parameters can be determined according to the thermodynamic Equations S10 and S11:

$$\Delta G^0 = -RT \ln K_c \quad (\text{Eq. S10})$$

The relationship between ΔG^0 and ΔH^0 is described as follows:

$$\Delta G^0 = \Delta H^0 - T \Delta S^0 \quad (\text{Eq. S11})$$

The well-known van't Hoff equation is obtained by substituting Equation S10 in Equation S11:

$$\ln K_c = \frac{-\Delta H^0}{R} \times \frac{1}{T} + \frac{\Delta S^0}{R} \quad (\text{Eq. S12})$$

The Gibbs energy change ΔG^0 is directly calculated from Equation 12, whereas the enthalpy change ΔH^0 and the entropy change ΔS^0 are determined from the slope and intercept, respectively, of a plot of $\ln K_c$ versus $1/T$ (Equation S12).

The parameter K_c can be obtained from Equation S13 when the Langmuir isotherm is assumed, and by Equation S14 when the Freundlich isotherm is assumed (Ghosal and Gupta, 2015; Tran et al., 2016).

$$K_c = 55.5 \times 10^6 \times K_L \quad (\text{Eq. S13})$$

where the factor 55.5 is the number of moles of pure water per liter, K_L is obtained by Equation S3 and K_c is dimensionless.

$$K_c = \frac{K_F \rho}{10^6} \left(\frac{10^6}{\rho} \right)^{\left(1 - \frac{1}{n} \right)} \quad (\text{Eq. S14})$$

where K_F ($\mu\text{mol g}^{-1}/(\mu\text{mol L}^{-1})^n$) is the Freundlich constant and n (dimensionless) is the Freundlich intensity parameter (obtained by Equation 6), R is the universal gas constant ($8.314 \text{ j mol}^{-1} \text{ K}^{-1}$), T is the absolute temperature in Kelvin, and ρ is the density of pure water (assumed as 1.0 g mL^{-1}).

Adsorption kinetics

The sorption kinetics were fitted by three models: nonlinear and linear forms of pseudo-first-order (PFO), nonlinear and linear forms of pseudo-second-order (PSO), and intraparticle diffusion (ID). These three models were correspondingly described as follows:

$$q_t = q_e(1 - e^{-k_1 t}) \quad (\text{Eq. S15})$$

$$\ln(q_e - q_t) = -k_1 t + \ln(q_e) \quad (\text{Eq. S16})$$

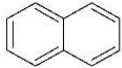
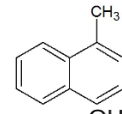
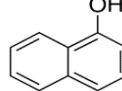
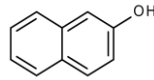
$$q_t = \frac{q_e^2 k_2 t}{1 + k_2 q_e t} \quad (\text{Eq. S17})$$

$$\frac{t}{q_t} = \left(\frac{1}{q_e}\right) t + \frac{1}{k_2 q_e^2} \quad (\text{Eq. S18})$$

$$qt = K_p \sqrt{t} + C \quad (\text{Eq. S19})$$

where q_t and q_e ($\mu\text{mol g}^{-1}$) are the amounts of Nap, Me-Nap, α -Naphthol and β -Naphthol removed at a determined time t (min) and in equilibrium, respectively, k_1 (min^{-1}), k_2 ($\text{g } \mu\text{mol min}^{-1}$) and k_p ($\mu\text{g g}^{-1} \text{min}^{1/2}$) are the values of constants of PFO, PSO and ID, respectively, and C ($\mu\text{mol g}^{-1}$) is a constant associated with boundary layer thickness.

Table 6. S1: Naphthalene and naphthalene derivatives physical and chemical properties.

PAH	Structure	Molecular Weight	MP (°C)	BP (°C)	Solubility (mg L ⁻¹)	LogK _{ow}	pKa	Cacinogenicity IARC/US EPA
Naphthalene		128.17	80.2	217.9	31	3.37	-	2B
1-Methylnaphthalene		142.2	30.4	244	28	3.87	-	NI
α -Naphthol		144.17	95	288	866	2.85	9.34	2B
β -Naphthol		144.17	123	285	755	2.7	9.51	2B

*IARC - International Agency for Research on Cancer; US EPA - Environmental Protection Agency; 2B= possible carcinogen for humans; NI= not included.

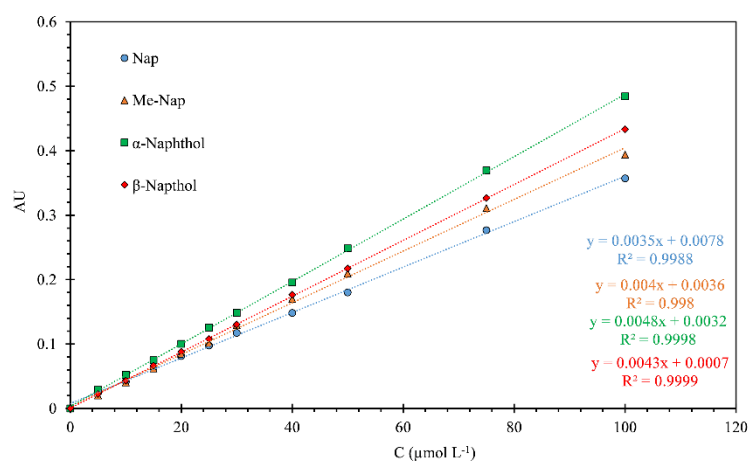


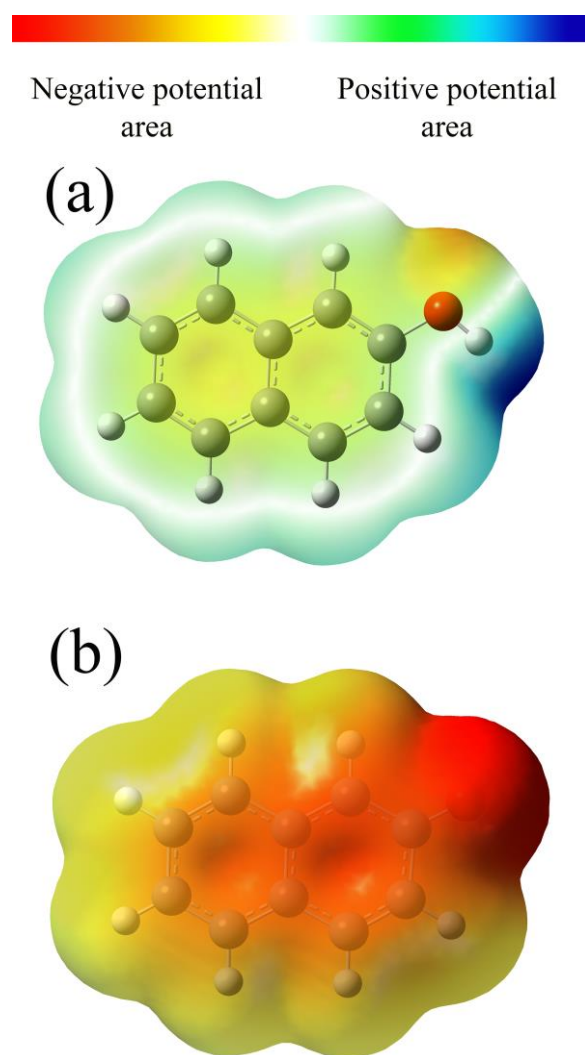
Figure 6. S1: Analytical curves for PAH studied.

Table 7. S2: Linear isotherm parameters.

Adsorbate	HDPE Adsorbent	Langmuir			Freundlich			Dubnin-Radushkevich		
		K_L (L μmol^{-1})	Q_{max} ($\mu\text{mol g}^{-1}$)	R^2	K_F ($\mu\text{mol g}^{-1} \mu\text{g L}^{-1}$)	n	R^2	q_{DR}	E (kJ μmol^{-1})	R^2
Nap	commercial	0.2111	21.65	0.8225	0.4529	0.0963	0.9911	55.46	43.85	0.91506
	waste	0.2849	17.33	0.7970	0.1963	1.2547	0.9902	30.19	87.71	0.9021
Me-Nap	commercial	0.0065	166.39	0.4489	0.9646	0.9355	0.9951	47.40	129.10	0.8419
	waste	0.0835	30.58	0.55	0.4464	0.6985	0.9801	36.63	84.52	0.9669
α -Naphthol	commercial	0.0472	41.32	0.9991	0.9526	1.3709	0.9837	26.22	54.23	0.9192
	waste	5.5609	1.32	0.9875	0.6087	3.4270	0.9432	1.23	91.29	0.5514

Table 8. S3: Relationship between isotherm parameters and curve type.

Freundlich exponent	Separation Factor	Isotherm shapes	Curve type
$n = 0$	$R_L = 0$	Irreversible	Horizontal
$n < 1$	$R_L < 1$	Favorable	Concave
$n = 1$	$R_L = 1$	Linear	Linear
$n > 1$	$R_L > 1$	Unfavorable	Convex

Figure 7. S2: (a) β -Naphthol; (b) β -Naphtholate.

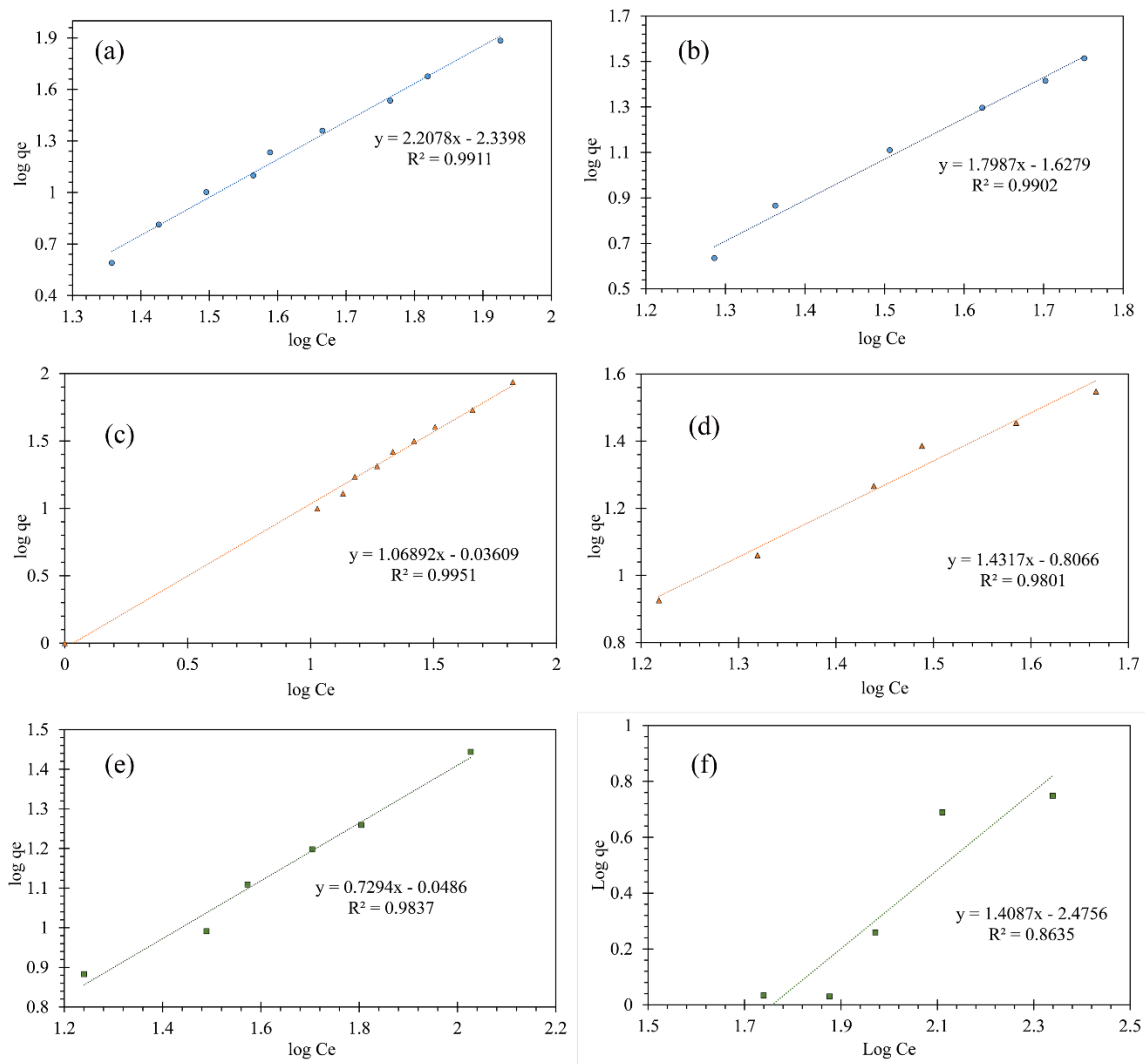


Figure 8. S3: Freundlich isotherm linear graph. (a) and (b) Naphthalene (blue balls) onto commercial and waste HDPE; (c) and (d) Me-Nap (orange triangles) onto commercial and waste HDPE; (e) and (f) α -Naphthol (green square) onto commercial and waste HDPE.

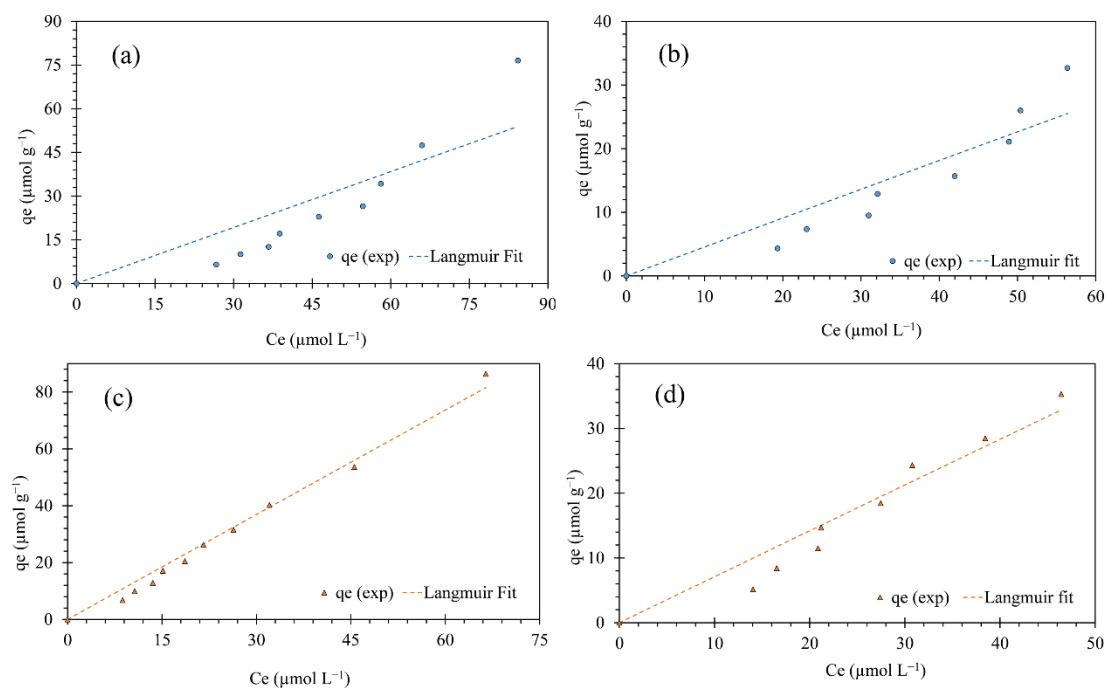


Figure 9. S4: Nonlinear Langmuir isotherms. (a) and (B) Nap onto commercial and waste HDPE; (b) and (c) Me-Nap onto commercial and waste HDPE.

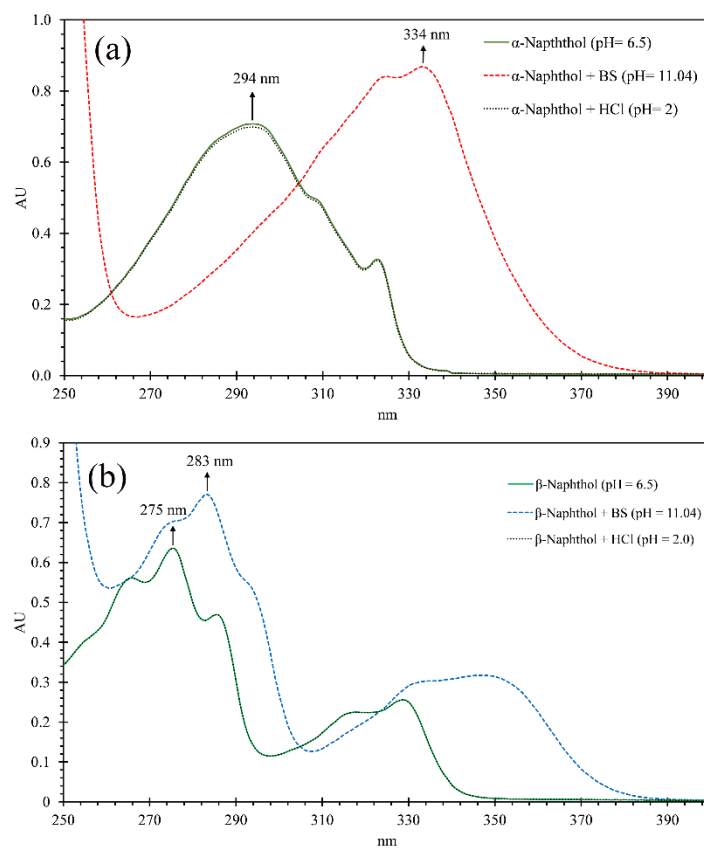


Figure 10. S5: Spectrum on different pH values. (a) α -Naphthol; (b) β -Naphthol.

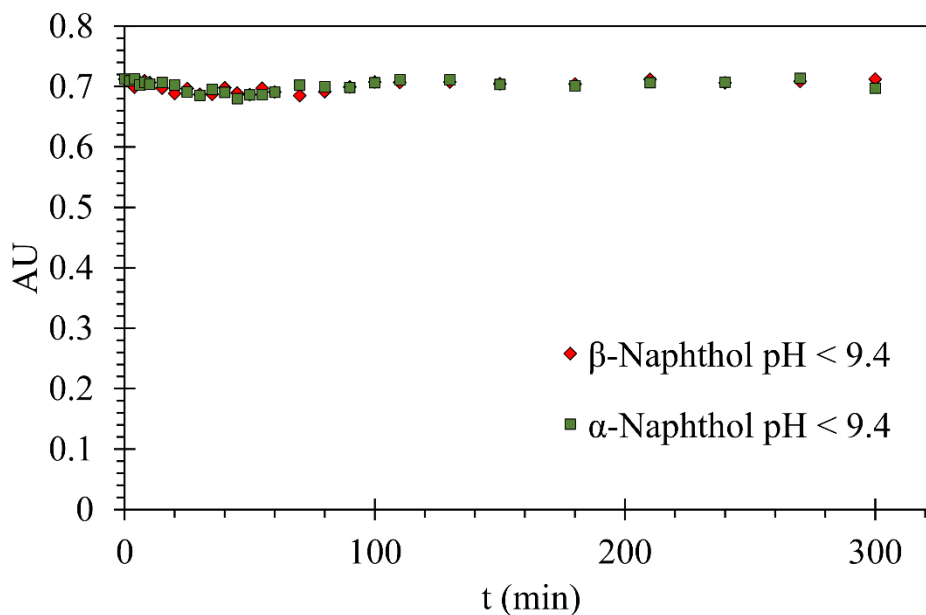


Figure 11. S6: α -Naphthol and β -Naphthol on pH < 9.4.

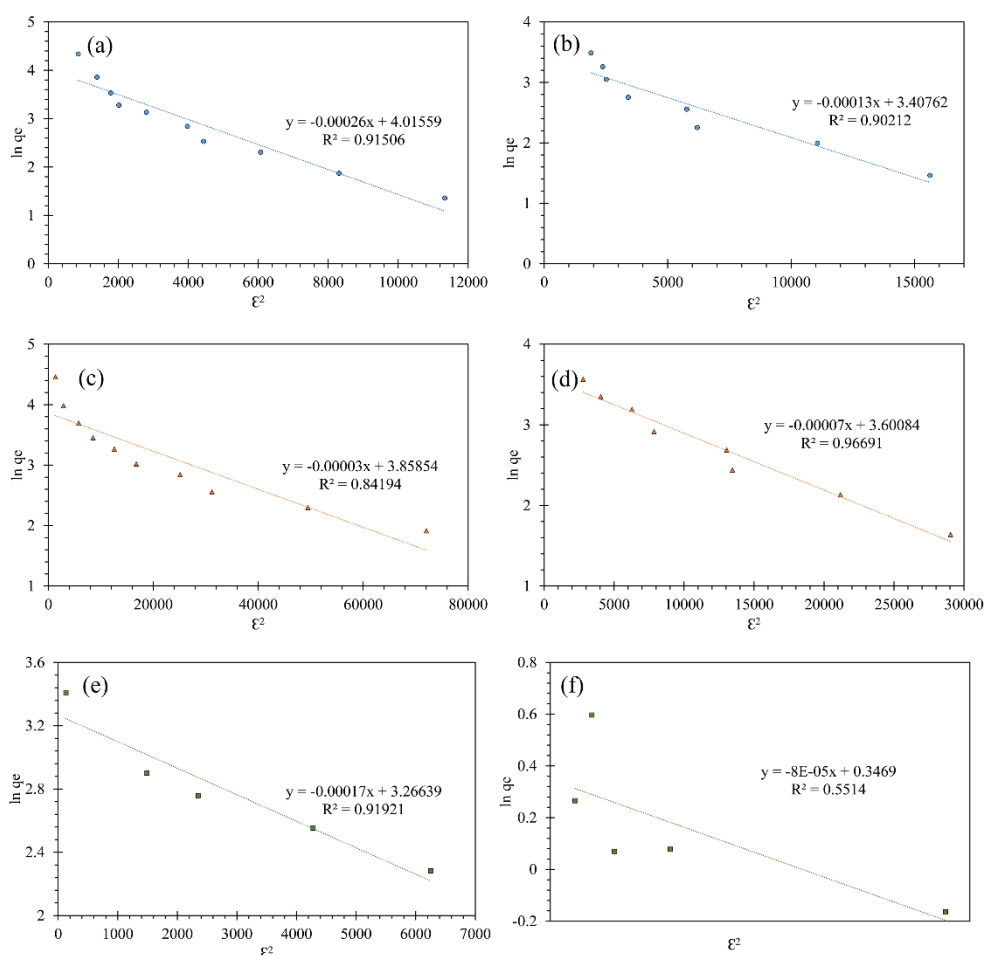


Figure 12. S7: Dubinin-Radushkevich linear isotherm. (a) and (b) Nap (blue balls) onto commercial and waste HDPE; (c) and (d) Me-Nap (orange triangles) onto commercial and waste HDPE (e) and (f) α -Naphthol (green square) onto commercial and waste HDPE.

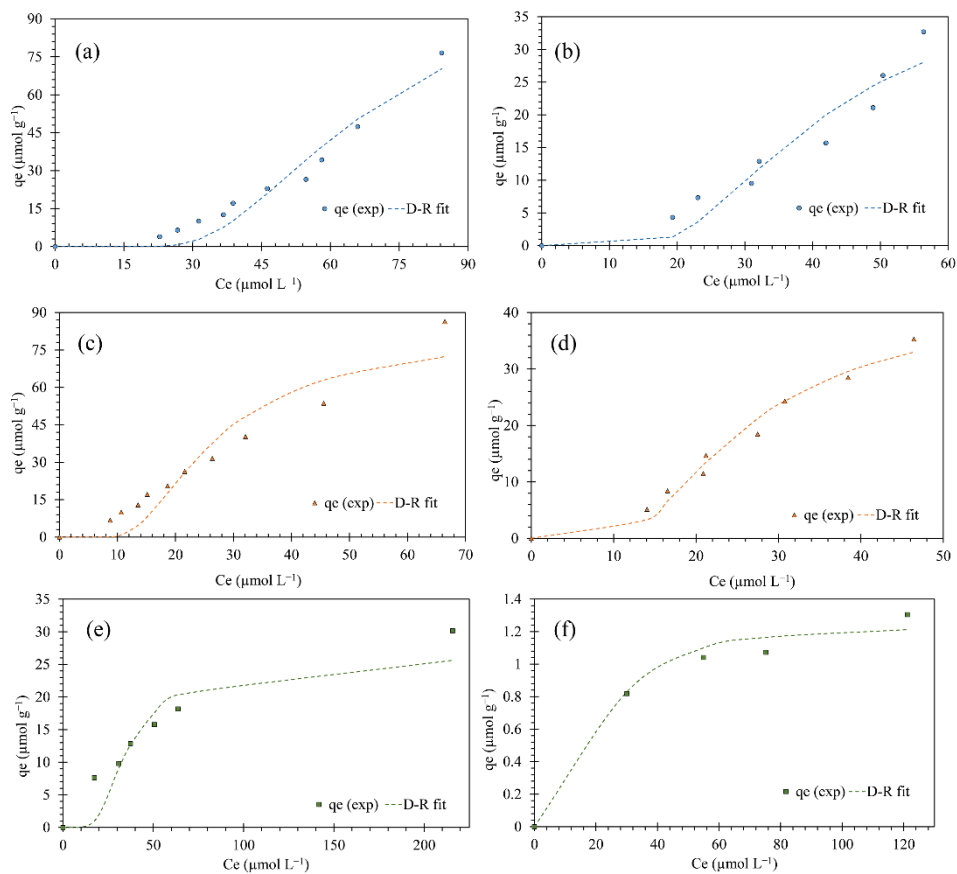


Figure 13. S8: Dubinin-Radushkevich nonlinear isotherm. (a) and (b) Nap (blue balls) onto commercial and waste HDPE; (c) and (d) Me-Nap (orange triangles) onto commercial and waste HDPE (e) and (f) α -Naphthol (green square) onto commercial and waste HDPE.

Table 9. S4: Thermodynamic parameters for adsorption of Nap and its derivatives onto commercial and waste HDPE.

Adsorbent HDPE	Adsorbate	Temperature (°C)	ΔG° (kJ mol ⁻¹)	ΔH° (kJ mol ⁻¹)	ΔS° (kJ mol ⁻¹)
Commercial	Nap	10	26.15	50.06	0.070
		25	28.71		
		35	29.61		
		45	33.00		
	Me-Nap	10	30.71	66.07	0.122
		25	31.19		
		35	32.20		
		45	26.48		
	α -Naphthol	10	-33.25	-43.71	-0.037
		25	-33.10		
		35	-32.25		
		45	-17.63		
Waste	Nap	10	36.22	77.17	0.145
		25	32.72		
		35	33.68		
		45	30.40		
	Me-Nap	10	66.45	64.63	0.103
		25	33.72		
		35	33.18		
		45	31.63		
	α -Naphthol	10	-37.32	-44.10	-0.025
		25	-35.93		
		35	-36.91		
		45	-38.26		

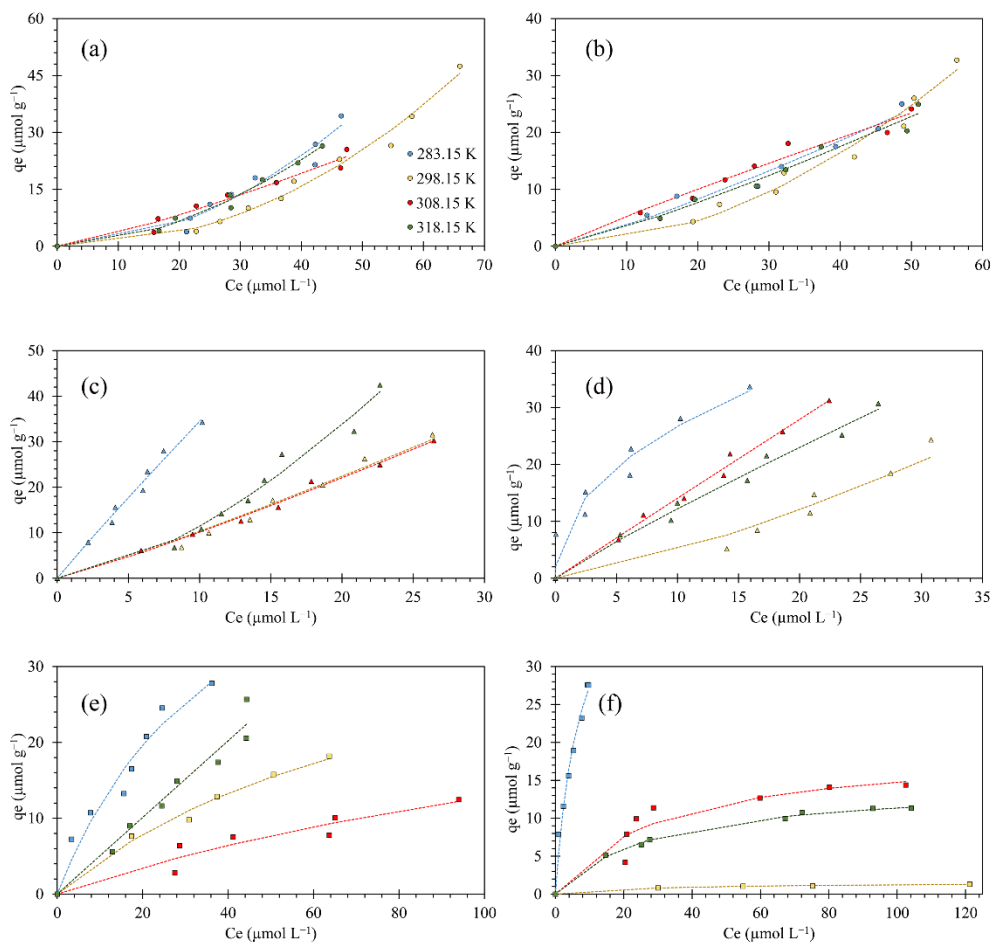


Figure 14. S9: Isotherm at different temperatures. (a) Nap onto HDPEc; (b) Nap onto HDPEw; (c) Me-Nap onto HDPEc; (d) Me-Nap onto HDPEw; (e) α -Naphthol onto HDPEc; (f) α -Naphthol onto HDPEw.

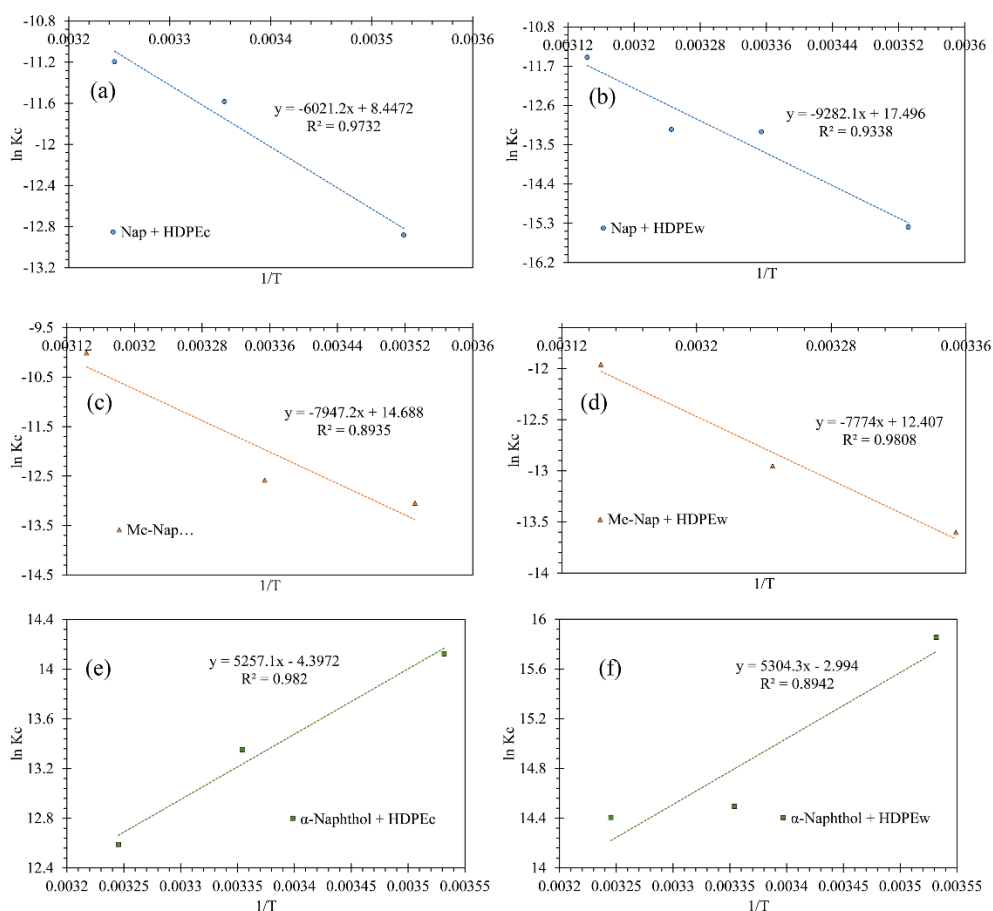


Figure 15. S10: Linear plot of $\ln K_c$ versus $1/T$ for the adsorption of PAHs on microplastics at different temperatures.

Table 10. S5: Nonlinear kinetic parameters for PAH

Adsorbate	Adsorbent HDPE	Pseudo-first-order		Pseudo-second-order		Diffusion-intraparticle model		
		k_1 (min^{-1})	q_e ($\mu\text{mol g}^{-1}$)	k_2 ($\text{g } \mu\text{mol}^{-1} \text{min}^{-1}$)	q_e ($\mu\text{mol g}^{-1}$)	k_p ($\mu\text{mol g}^{-1} \text{min}^{-1/2}$)	C ($\mu\text{mol g}^{-1}$)	R^2
Nap	commercial	0.1463	14.93	0.015	15.88	0.5354	9.08	0.5074
	Waste	0.086	17.32	0.007	18.93	0.8620	7.75	0.7672
Me-Nap	commercial	0.2579	25.23	0.017	26.29	0.7666	17.09	0.4313
	Waste	0.0411	22.17	0.045	23.67	1.2157	7.34	0.7825
α -Naphthol	commercial	0.0068	13.69	0.00024	20.33	0.7734	-1.16	0.9811
	Waste	0.0052	8.57	0.00027	13.08	0.4179	-0.63	0.9787

Table 11. S6: Linear kinetic parameters

Adsorbate	HDPE Adsorbent	Pseudo-first-order			Pseudo-second-order			Diffusion-intraparticle mode		
		K_1 (min^{-1})	q_e ($\mu\text{mol g}^{-1}$)	R^2	K_2 ($\text{g } \mu\text{mol}^{-1} \text{min}^{-1}$)	q_e ($\mu\text{mol g}^{-1}$)	R^2	K_p ($\mu\text{mol g}^{-1} \text{min}^{-1/2}$)	C ($\mu\text{mol g}^{-1}$)	R^2
Nap	commercial	0.6870	11.10	0.9490	0.0148	15.87	0.9995	0.5354	9.08	0.5074
	waste	0.0376	14.34	0.9030	0.0079	17.92	0.9980	0.8620	7.75	0.7672
Me-Nap	commercial	0.0614	14.41	0.8142	0.0181	26.16	0.9999	0.7666	17.09	0.4313
	waste	0.0365	21.60	0.9658	0.0028	24.14	0.9987	1.2157	7.34	0.7825
α -Naphthol	commercial	0.0081	10.57	0.9205	0.0005	16.53	0.8104	0.7734	-1.16	0.9811
	waste	0.0053	6.79	0.8549	0.0009	8.76	0.7781	0.4179	-0.6331	0.9787

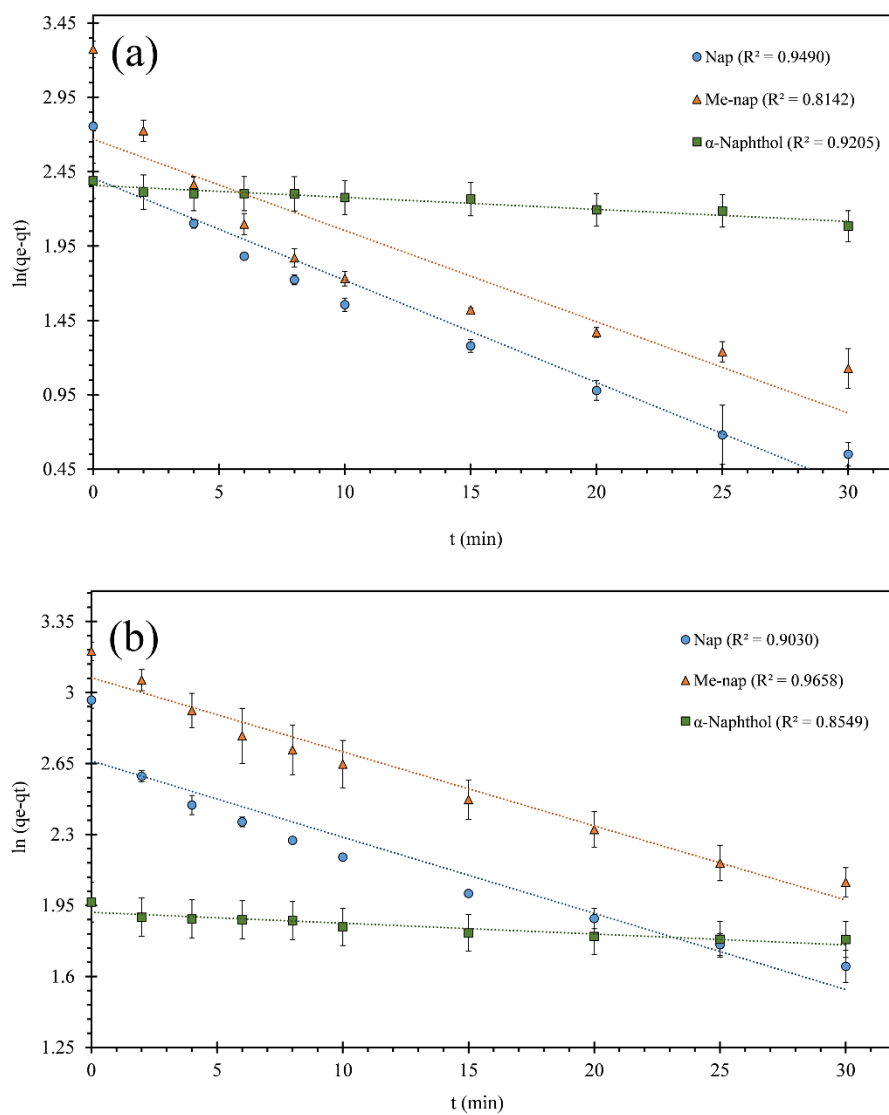


Figure 16. S11: Pseudo-first order linear graph. (a) PAHs onto commercial HDPE; (b) PAHs onto waste HDPE.

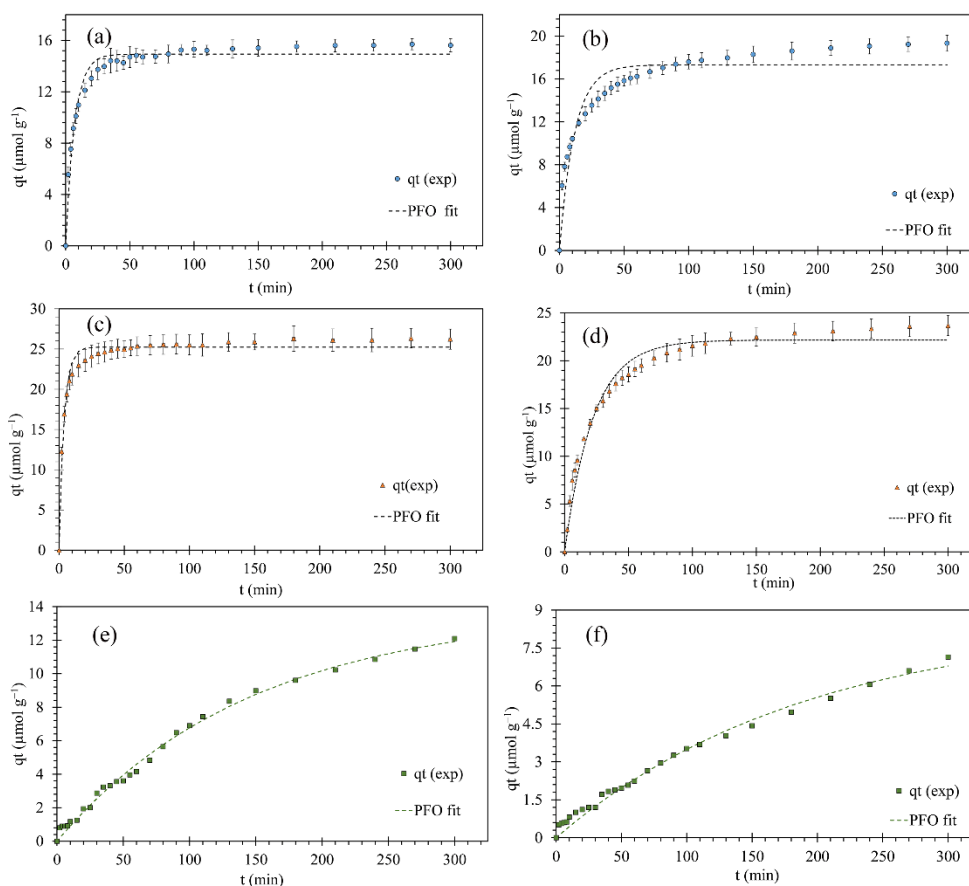


Figure 17. S12: Pseudo-first order nonlinear graph. (a) Nap onto commercial HDPE; (b) Nap onto waste HDPE; (c) Me-Nap onto commercial HDPE; (d) Me-Nap onto waste HDPE; (e) α -Naphthol onto commercial HDPE; (f) α -Naphthol onto waste HDPE.

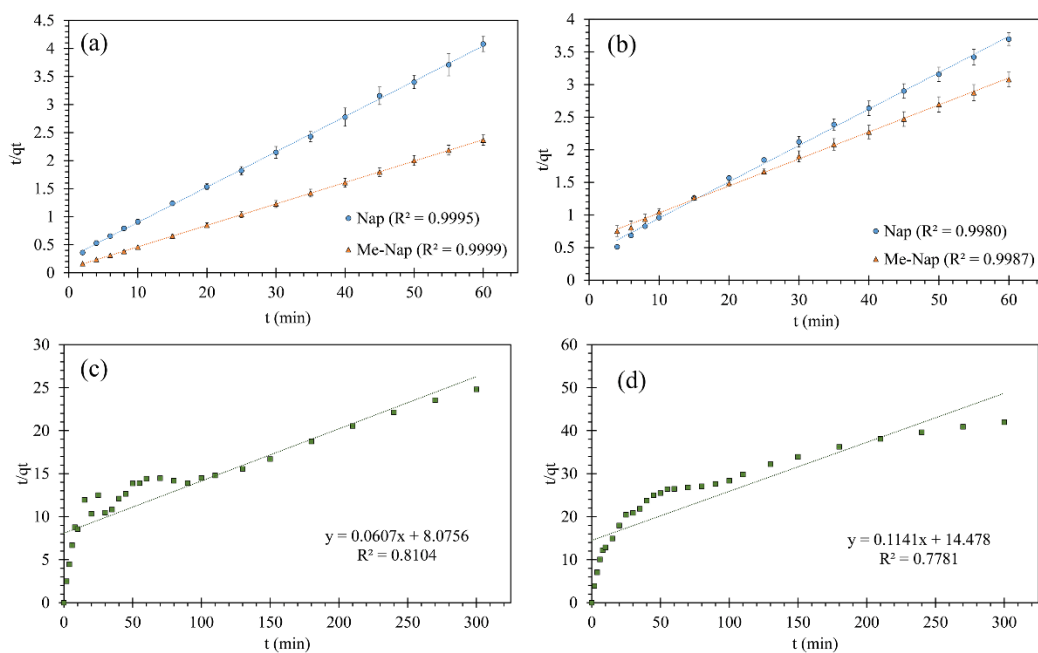


Figure 18. S13: Pseudo-second order linear graph. (a) Nap and Me-Nap onto commercial HDPE; (b) Nap and Me-Nap onto waste HDPE. (c) α -Naphthol onto commercial HDPE; (d) α -Naphthol onto waste HDPE.

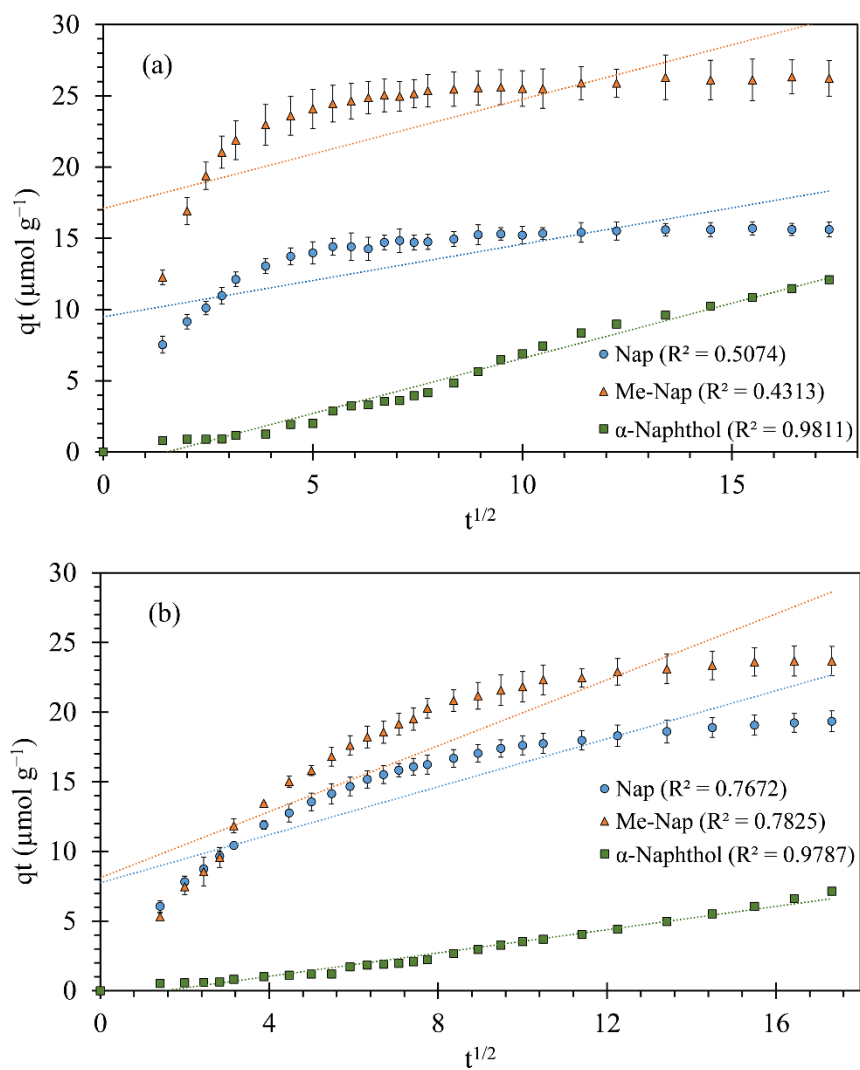


Figure 19. S14: Intraparticle diffusion plot. (a) adsorption of Nap, Me-Nap and α -Naphthol onto commercial HDPE. (b) adsorption of Nap, Me-Nap and α -Naphthol onto waste HDPE.

CHAPTER III- General Conclusions

Adsorption study involving PAH and polymers is recurrent and seriously explored on over decades Adsorption studies involving PAH and polymers are recurrent in the literature and have been seriously explored over decades. Several polymer types (e.g., PE, PS, PET, PVC) have been were reported as capable of adsorbing and carrying different organic compounds. Research using commercial polymers and different organic molecules are being constantly published. However, based on the current literature, little is reported about the influence of functional groups on PAH and the use of waste polymers, thus, it was possible to verify the existence of this gap. Therefore, adsorption studies with HPA derivatives using residual polymers in comparison with commercial plastic, aiming to approximate what happens in the real environmental is what this work has developed.

This work showed the utilization of naphthalene derivatives with methyl ($-CH_3$) and hydroxyl ($-OH$) groups and their influence on adsorption behavior. Chapter II showed how the presence of these charged and uncharged groups are able to change the properties and characteristics of the nap molecule. The adsorption assays showed different behaviors comparing Nap derivatives with methyl with the ones with hydroxyl groups in it, regarding computational, isothermal, thermodynamic and kinetic studies. The findings indicate that nonpolar molecules have a higher adsorption capacity compared to polar molecules, corroborated by the LogKow values. The high hydrophobicity of both adsorbent-adsorbate favor the hydrophobic interactions and increases adsorption capacity (qe).

The high molecular polarity caused by the hydroxyl groups in α -Naphthol inhibited LogKow, resulting in a low adsorption capacity on HDPE microplastics. By ESP analysis, the interaction mechanism involving Nap and apolar derivatives with both HDPE is mostly composed of hydrophobic interactions and π - π interactions. In contrast, in nonpolar derivatives, the main interactions result from van der Walls forces and H bonds. Furthermore, Nap and Me-Nap have an unfavorable isotherm, whereas α -Naphthol has a favorable adsorption isotherm. The thermodynamic study showed that polar ($-OH$) functional groups make PAH adsorption favorable under increase temperatures and ($-CH_3$) functional group is favor with decrease temperature The adsorption kinetics study presented a non-linear pseudo-second order model for all cases and the non-polar derived

compound (Me-Nap) has a higher kinetic constant value compared to Nap and α -Naphthol.

This study provides new insight into the affinity of PAH derivatives with microplastics, which therefore improves our understanding of the environmental fates of microplastics and organic pollutants by mean of a physical-chemical study.

References

- Alaee, M., Whittal, R.M., Strachan, W.M.J., 1996. The effect of water temperature and composition on Henry's law constant for various PAH's. *Chemosphere*. 32, 1153–1164. [https://doi.org/10.1016/0045-6535\(96\)00031-8](https://doi.org/10.1016/0045-6535(96)00031-8).
- Amato-Lourenço, L.F., Carvalho-Oliveira, R., Júnior, G.R., dos Santos Galvão, L., Ando, R.A., Mauad, T., 2021. Presence of airborne microplastics in human lung tissue. *J. Hazard. Mater.* 416, 126124. <https://doi.org/10.1016/j.jhazmat.2021.126124>.
- Anastopoulos, I., Kyzas, G.Z., 2016. Are the thermodynamic parameters correctly estimated in liquid-phase adsorption phenomena? *J. Mol. Liq.* 218, 174–185. <https://doi.org/10.1016/j.molliq.2016.02.059>.
- Andrady, A.L., 2017. The plastic in microplastics: A review. *Mar. Pollut. Bull.* 119, 12–22. <https://doi.org/10.1016/j.marpolbul.2017.01.082>.
- Bai, Y. et al. Occurrence, distribution, environmental risk assessment and source apportionment of polycyclic aromatic hydrocarbons (PAHs) in water and sediments of the Liaohe River Basin, China. *Bull. Environ. Contam. Toxicol.*, v. 93, n. 6, p. 744-51, 2014.
- Bansal, V., & Kim, K. H. (2015). Review of PAH contamination in food products and their health hazards. In *Environment International* (Vol. 84, pp. 26–38). Elsevier Ltd. <https://doi.org/10.1016/j.envint.2015.06.016>.
- Beriro, D. J., Cave, M. R., Wragg, J., Thomas, R., Wills, G., & Evans, F. (2016). A review of the current state of the art of physiologically-based tests for measuring human dermal in vitro bioavailability of polycyclic aromatic hydrocarbons (PAH) in soil. In *Journal of Hazardous Materials* (Vol. 305, pp. 240–259). Elsevier B.V. <https://doi.org/10.1016/j.jhazmat.2015.11.010>.
- Bullen, J.C., Saleesongsom, S., Gallagher, K., Weiss, D.J., 2021. A Revised Pseudo-Second-Order Kinetic Model for Adsorption, Sensitive to Changes in Adsorbate and Adsorbent Concentrations. *Langmuir*. 37, 3189–3201. <https://doi.org/10.1021/acs.langmuir.1c00142>.
- Bytingsvik, J., Parkerton, T.F., Guyomarch, J., Tassara, L., LeFloch, S., Arnold, W.R., Brander, S.M., Volety, A., Camus, L., 2020. The sensitivity of the deepsea species northern shrimp (*Pandalus borealis*) and the cold-water coral (*Lophelia pertusa*) to oil-associated aromatic compounds, dispersant, and Alaskan North Slope crude oil. *Mar. Pollut. Bull.* 156, 111202. <https://doi.org/10.1016/j.marpolbul.2020.111202>.

- Chen, X., Hossain, M.F., Duan, C., Lu, J., Tsang, Y.F., Islam, M.S., Zhou, Y., 2022. Isotherm models for adsorption of heavy metals from water - A review. *Chemosphere*. 307, 135545. <https://doi.org/10.1016/j.chemosphere.2022.135545>.
- Coyle, R., Hardiman, G., Driscoll, K.O., 2020. Microplastics in the marine environment: A review of their sources, distribution processes, uptake and exchange in ecosystems. *C. Studies in Chem. and Environ. Eng.* 2, 100010. <https://doi.org/10.1016/j.cscee.2020.100010>.
- Dilshad, A., Taneez, M., Younas, F., Jabeen, A., Rafiq, M.T., Fatimah, H., 2022. Microplastic pollution in the surface water and sediments from Kallar Kahar wetland, Pakistan: occurrence, distribution, and characterization by ATR-FTIR. *Environ. Monit. Assess.* 194, 511. <https://doi.org/10.1007/s10661-022-10171-z>.
- Ding, X., Jiao, W., Yang, Y., Zeng, Z., Huang, Z., 2021. Effects of oxygenated groups on the adsorption removal of dibenzofuran by activated coke: Experimental and DFT studies. *J Environ. Chem. Eng.* 9, 106775. <https://doi.org/10.1016/j.jece.2021.106775>.
- Ekvall, M.T., Gimskog, I., Hua, J., Kelpsiene, E., Lundqvist, M., Cedervall, T., 2022. Size fractionation of high-density polyethylene breakdown nanoplastics reveals different toxic response in *Daphnia magna*. *Sci. Rep.* 12, 3109. <https://doi.org/10.1038/s41598-022-06991-1>.
- Ewa, B., Danuta, M.-Š., 2017. Polycyclic aromatic hydrocarbons and PAH-related DNA adducts. *J. Appl. Genet.* 58, 321–330. <https://doi.org/10.1007/s13353-016-0380-3>.
- Farombi, E. O., Ajayi, B. O., & Adedara, I. A. (2020). 6-Gingerol delays tumorigenesis in benzo[a]pyrene and dextran sulphate sodium-induced colorectal cancer in mice. *Food and Chemical Toxicology*, 142. <https://doi.org/10.1016/j.fct.2020.111483>.
- Ferguson, K. K., McElrath, T. F., Pace, G. G., Weller, D., Zeng, L., Pennathur, S., Cantonwine, D. E., & Meeker, J. D. (2017). Urinary Polycyclic Aromatic Hydrocarbon Metabolite Associations with Biomarkers of Inflammation, Angiogenesis, and Oxidative Stress in Pregnant Women. *Environmental Science & Technology*, 51(8), 4652–4660. <https://doi.org/10.1021/acs.est.7b01252>.
- Finlayson-Pitts, B. J.; James N. Pitts, J. *Upper and Lower Atmosphere*. 1st. San Diego, US: Academic Press, 2000.
- Fisicaro, E., Compari, C., Braibanti, A., 2004. Entropy/enthalpy compensation: hydrophobic effect, micelles and protein complexes. *Physic. Chem. Chem. Physic.* 6, 4156-4166. <https://doi.org/10.1039/b404327h>.

- Franco, C.A., Nassar, N.N., Cortés, F.B., 2014. Removal of oil from oil-in-saltwater emulsions by adsorption onto nano-alumina functionalized with petroleum vacuum residue. *J. Colloid. Interface Sci.* 433, 58–67. <https://doi.org/10.1016/j.jcis.2014.07.011>.
- Fu, L., Li, J., Wang, G., Luan, Y., Dai, W., 2021. Adsorption behavior of organic pollutants on microplastics. *Ecotoxicol. Environ. Saf.* 217, 112207. <https://doi.org/10.1016/j.ecoenv.2021.112207>.
- Furukawa, T., Sato, H., Kita, Y., Matsukawa, K., Yamaguchi, H., Ochiai, S., Siesler, H.W., Ozaki, Y., 2006. Molecular Structure, Crystallinity and Morphology of Polyethylene/Polypropylene Blends Studied by Raman Mapping, Scanning Electron Microscopy, Wide Angle X-Ray Diffraction, and Differential Scanning Calorimetry. *Polym. J.* 38, 1127–1136. <https://doi.org/10.1295/polymj.PJ2006056>.
- Galarneau, E. (2008). Source specificity and atmospheric processing of airborne PAHs: Implications for source apportionment. In *Atmospheric Environment* (Vol. 42, Issue 35, pp. 8139–8149). <https://doi.org/10.1016/j.atmosenv.2008.07.025>
- González-López, M.E., Laureano-Anzaldo, C.M., Pérez-Fonseca, A.A., Arellano, M., Robledo-Ortíz, J.R., 2022. A Critical Overview of Adsorption Models Linearization: Methodological and Statistical Inconsistencies. *Sep. Purif. Rev.* 51, 358–372. <https://doi.org/10.1080/15422119.2021.1951757>.
- Horton, A.A., Walton, A., Spurgeon, D.J., Lahive, E., Svendsen, C., 2017. Microplastics in freshwater and terrestrial environments: Evaluating the current understanding to identify the knowledge gaps and future research priorities. *Sci. Total Environ.* 586, 127–141. <https://doi.org/10.1016/j.scitotenv.2017.01.190>.
- Hu, Q., Pang, S., Wang, D., 2022. In-depth Insights into Mathematical Characteristics, Selection Criteria and Common Mistakes of Adsorption Kinetic Models: A Critical Review. *Sep. Purif. Rev.* 51, 281–299. <https://doi.org/10.1080/15422119.2021.1922444>.
- Hüffer, T., Hofmann, T., 2016. Sorption of non-polar organic compounds by micro-sized plastic particles in aqueous solution. *Environ. Pollut.* 214, 194–201. <https://doi.org/10.1016/j.envpol.2016.04.018>.
- Issac, M.N., Kandasubramanian, B., 2021. Effect of microplastics in water and aquatic systems. *Environ. Sci. Pollut. Res.* 28, 19544–19562. <https://doi.org/10.1007/s11356-021-13184-2>.
- Jedrychowski, Wiesław A., et al. "Prenatal exposure to polycyclic aromatic hydrocarbons and cognitive dysfunction in children." *Environmental Science and Pollution Research* 22.5 (2015): 3631-3639.

- Jiang, Z., Huang, L., Fan, Y., Zhou, S., Zou, X., 2022. Contrasting effects of microplastic aging upon the adsorption of sulfonamides and its mechanism. *Chem. Eng. J.* 430, 132939. <https://doi.org/10.1016/j.cej.2021.132939>.
- Jomova, K., Baros, S., Valko, M., 2012. Redox active metal-induced oxidative stress in biological systems. *Transit. Met. Chem.* 37, 127–134. <https://doi.org/10.1007/s11243-012-9583-6>.
- Kane, I.A., Clare, M.A., 2019. Dispersion, Accumulation, and the Ultimate Fate of Microplastics in Deep-Marine Environments: A Review and Future Directions. *Front. Earth Sci. (Lausanne)* 7. <https://doi.org/10.3389/feart.2019.00080>.
- Karlsson, T.M., Kärrman, A., Rotander, A., Hassellöv, M., 2020. Comparison between manta trawl and in situ pump filtration methods, and guidance for visual identification of microplastics in surface waters. *Environ. Sci. Pollut. Res.* 27, 5559–5571. <https://doi.org/10.1007/s11356-019-07274-5>.
- Kim, M., Kennicutt, M.C., Qian, Y., 2008. Source characterization using compound composition and stable carbon isotope ratio of PAHs in sediments from lakes, harbor, and shipping waterway. *Sci. Total Environ.* 389, 367–377. <https://doi.org/10.1016/j.scitotenv.2007.08.045>.
- Kinigopoulou, V., Pashalidis, I., Kalderis, D., Anastopoulos, I., 2022. Microplastics as carriers of inorganic and organic contaminants in the environment: A review of recent progress. *J. Mol. Liq.* 350, 118580. <https://doi.org/10.1016/j.molliq.2022.118580>.
- Kronberg, B., 2016. The hydrophobic effect. *Curr. Opin. Colloid. Interface Sci.* 22, 14–22. <https://doi.org/10.1016/j.cocis.2016.02.001>.
- Li, H., Wang, F., Li, J., Deng, S., Zhang, S., 2021. Adsorption of three pesticides on polyethylene microplastics in aqueous solutions: Kinetics, isotherms, thermodynamics, and molecular dynamics simulation. *Chemosphere.* 264, 128556. <https://doi.org/10.1016/j.chemosphere.2020.128556>.
- Lim, Y.-S., Kim, J.-H., 2017. Isotherm, kinetic and thermodynamic studies on the adsorption of 13-dehydroxybaccatin III from *Taxus chinensis* onto *Sylopute*. *J. Chem. Thermodyn.* 115, 261–268. <https://doi.org/10.1016/j.jct.2017.08.009>.
- Lin, C.Y., Wheelock, Å.M., Morin, D., Baldwin, R.M., Lee, M.G., Taff, A., Plopper, C., Buckpitt, A., Rohde, A., 2009. Toxicity and metabolism of methylnaphthalenes: Comparison with naphthalene and 1-nitronaphthalene. *Toxicology.* 260, 16–27. <https://doi.org/10.1016/j.tox.2009.03.002>.

- Liu, K., Wang, X., Fang, T., Xu, P., Zhu, L., Li, D., 2019. Source and potential risk assessment of suspended atmospheric microplastics in Shanghai. *Sci. Total Environ.* 675, 462–471. <https://doi.org/10.1016/j.scitotenv.2019.04.110>.
- Long, C., Li, A., Wu, H., Zhang, Q., 2009. Adsorption of naphthalene onto macroporous and hypercrosslinked polymeric adsorbent: Effect of pore structure of adsorbents on thermodynamic and kinetic properties. *Colloids Surf. A. Physicochem. Eng. Asp.* 333, 150–155. <https://doi.org/10.1016/j.colsurfa.2008.09.037>.
- Lu, T., Chen, F., 2012. Multiwfn: A multifunctional wavefunction analyzer. *J. Comput. Chem.* 33, 580–592. <https://doi.org/10.1002/jcc.22885>.
- Luo, H., Liu, C., He, D., Xu, J., Sun, J., Li, J., Pan, X., 2022. Environmental behaviors of microplastics in aquatic systems: A systematic review on degradation, adsorption, toxicity and biofilm under aging conditions. *J. Hazard. Mater.* 423, 126915. <https://doi.org/10.1016/j.jhazmat.2021.126915>.
- Mai, L., Bao, L.J., Shi, L., Liu, L.Y., Zeng, E.Y., 2018. Polycyclic aromatic hydrocarbons affiliated with microplastics in surface waters of Bohai and Huanghai Seas, China. *Environ. Pollut.* 241, 834–840. <https://doi.org/10.1016/j.envpol.2018.06.012>.
- Manzetti, S. Polycyclic Aromatic Hydrocarbons in the Environment: Environmental Fate and Transformation. *Polycyclic Aromat. Compd.*, v. 33, n. 4, p. 311-330, 2013.
- Mateos-Cárdenas, A., van Pelt, F.N.A.M., O'Halloran, J., Jansen, M.A.K., 2021. Adsorption, uptake and toxicity of micro- and nanoplastics: Effects on terrestrial plants and aquatic macrophytes. *Environ. Pollut.* 284, 117183. <https://doi.org/10.1016/j.envpol.2021.117183>.
- Mei, W., Chen, G., Bao, J., Song, M., Li, Y., Luo, C., 2020. Interactions between microplastics and organic compounds in aquatic environments: A mini review. *Sci. Total Environ.* 736, 139472. <https://doi.org/10.1016/j.scitotenv.2020.139472>.
- Menezes, H. C., de Barcelos, S. M. R., Macedo, D. F. D., Purceno, A. D., Machado, B. F., Teixeira, A. P. C., Lago, R. M., Serp, P., & Cardeal, Z. L. (2015). Magnetic N-doped carbon nanotubes: A versatile and efficient material for the determination of polycyclic aromatic hydrocarbons in environmental water samples. *Analytica Chimica Acta*, 873, 51–56. <https://doi.org/10.1016/j.aca.2015.02.063>
- Meng, X., Li, H., Zhang, Y., Cao, H., Sheng, Y., 2016. Analysis of polycyclic aromatic hydrocarbons (PAHs) and their adsorption characteristics on activated sludge during biological treatment of coking wastewater. *Desalination Water Treat.* 57, 23633–23643. <https://doi.org/10.1080/19443994.2015.1137233>.

- Moorthy, B., Chu, C., Carlin, D.J., 2015. Polycyclic aromatic hydrocarbons: From metabolism to lung cancer. *Toxic. Sci.* <https://doi.org/10.1093/toxsci/kfv040>.
- Nam, S.-W., Choi, D.-J., Kim, S.-K., Her, N., Zoh, K.-D., 2014. Adsorption characteristics of selected hydrophilic and hydrophobic micropollutants in water using activated carbon. *J. Hazard. Mater.* 270, 144–152. <https://doi.org/10.1016/j.jhazmat.2014.01.037>.
- Nassar, N.N., Arar, L.A., Marei, N.N., Abu Ghanim, M.M., Dwekat, M.S., Sawalha, S.H., 2014. Treatment of olive mill based wastewater by means of magnetic nanoparticles: Decolourization, dephenolization and COD removal. *Environ. Nanotechnol. Monit. Manag.* 1–2, 14–23. <https://doi.org/10.1016/j.enmm.2014.09.001>.
- Nielsen, K., Kalmykova, Y., Strömvall, A. M., Baun, A., & Eriksson, E. (2015). Particle phase distribution of polycyclic aromatic hydrocarbons in stormwater - Using humic acid and iron nano-sized colloids as test particles. *Science of the Total Environment*, 532, 103–111. <https://doi.org/10.1016/j.scitotenv.2015.05.093>
- Prajapati, A., Narayan Vaidya, A., Kumar, A.R., 2022. Microplastic properties and their interaction with hydrophobic organic contaminants: a review. *Environ. Sci. Pollut. Res.* 29, 49490–49512. <https://doi.org/10.1007/s11356-022-20723-y>.
- Qin, C., Hu, X., Waigi, M.G., Yang, B., Gao, Y., 2020. Amino and hydroxy substitution influences pyrene–DNA binding. *Sci. Total Environ.* 725, 138542. <https://doi.org/10.1016/j.scitotenv.2020.138542>.
- Rahim, M., Abu, N., Mas Haris, M.R.H., 2016. The effect of pH on the slow-release behaviour of 1- and 2-naphthol from chitosan film. *Cogent. Chem.* 2, 1234345. <https://doi.org/10.1080/23312009.2016.1234345>.
- Ruby, M. v., & Lowney, Y. W. (2012). Selective soil particle adherence to hands: Implications for understanding oral exposure to soil contaminants. In *Environmental Science and Technology* (Vol. 46, Issue 23, pp. 12759–12771). <https://doi.org/10.1021/es302473q>.
- Saad, A.A., Hussein, T., El-Sikaily, A., Abdel-Mohsen, M.A., Mokhamer, E.-H., Youssef, A.I., Mohammed, J., 2019. Effect of Polycyclic Aromatic Hydrocarbons Exposure on Sperm DNA in Idiopathic Male Infertility. *J. Health Pollut.* 9, 190309. <https://doi.org/10.5696/2156-9614-9.21.190309>.
- Saleh, T.A., Sari, A., Tuzen, M., 2022. Simultaneous removal of polyaromatic hydrocarbons from water using polymer modified carbon. *Biomass Convers Biorefin.* <https://doi.org/10.1007/s13399-021-02163-9>.

- Sato, H., Shimoyama, M., Kamiya, T., Amari, T., Šašić, S., Ninomiya, T., Siesler, H.W., Ozaki, Y., 2002. Raman spectra of high-density, low-density, and linear low-density polyethylene pellets and prediction of their physical properties by multivariate data analysis. *J. Appl. Polym. Sci.* 86, 443–448. <https://doi.org/10.1002/app.10999>.
- Schwarz, A.E., Ligthart, T.N., Boukris, E., van Harmelen, T., 2019. Sources, transport, and accumulation of different types of plastic litter in aquatic environments: A review study. *Mar. Pollut. Bull.* 143, 92–100. <https://doi.org/10.1016/j.marpolbul.2019.04.029>.
- Sexton, K., Salinas, J.J., McDonald, T.J., Gowen, R.M.Z., Miller, R.P., McCormick, J.B., Fisher-Hoch, S.P., 2011. Polycyclic aromatic hydrocarbons in maternal and umbilical cord blood from pregnant Hispanic women living in Brownsville, Texas. *Int. J. Environ. Res. Public Health.* 8, 3365–3379. <https://doi.org/10.3390/ijerph8083365>.
- Smith, B., 2018. *Infrared Spectral Interpretation*. CRC Press. <https://doi.org/10.1201/9780203750841>.
- Sørensen, L., Rogers, E., Altin, D., Salaberria, I., Booth, A.M., 2020. Sorption of PAHs to microplastic and their bioavailability and toxicity to marine copepods under co-exposure conditions. *Environ. Pollut.* 258. <https://doi.org/10.1016/j.envpol.2019.113844>.
- Strobl, G.R., Hagedorn, W., 1978. Raman spectroscopic method for determining the crystallinity of polyethylene. *J. Polym. Sci.: Polym. Physic. Edit.* 16, 1181–1193. <https://doi.org/10.1002/pol.1978.180160704>.
- Syamala, P.P.N., Würthner, F., 2020. Modulation of the Self-Assembly of π -Amphiphiles in Water from Enthalpy- to Entropy-Driven by Enwrapping Substituents. *Chem. – A European J.* 26, 8426–8434. <https://doi.org/10.1002/chem.202000995>.
- Szewc, K., Graca, B., Dołęga, A., 2021. Atmospheric deposition of microplastics in the coastal zone: Characteristics and relationship with meteorological factors. *Sci. Total Environ.* 761, 143272. <https://doi.org/10.1016/j.scitotenv.2020.143272>.
- Thommes, M., Kaneko, K., Neimark, A. v., Olivier, J.P., Rodriguez-Reinoso, F., Rouquerol, J., Sing, K.S.W., 2015. Physisorption of gases, with special reference to the evaluation of surface area and pore size distribution (IUPAC Technical Report). *Pure Appl. Chem.* 87, 1051–1069. <https://doi.org/10.1515/pac-2014-1117>.
- Torres, F.G., Dioses-Salinas, D.C., Pizarro-Ortega, C.I., De-la-Torre, G.E., 2021. Sorption of chemical contaminants on degradable and non-degradable microplastics: Recent progress and research trends. *Sci. Total Environ.* <https://doi.org/10.1016/j.scitotenv.2020.143875>.

- Tran, H.N., You, S.-J., Hosseini-Bandegharai, A., Chao, H.-P., 2017. Mistakes and inconsistencies regarding adsorption of contaminants from aqueous solutions: A critical review. *Water Res.* 120, 88–116. <https://doi.org/10.1016/j.watres.2017.04.014>.
- Velez, J.F.M., Shashoua, Y., Syberg, K., Khan, F.R., 2018. Considerations on the use of equilibrium models for the characterisation of HOC-microplastic interactions in vector studies. *Chemosphere.* 210, 359–365. <https://doi.org/10.1016/j.chemosphere.2018.07.020>.
- Vecchiato, M. et al. Persistent Organic Pollutants (POPs) in Antarctica: Occurrence in continental and coastal surface snow. *Microchem. J.*, v. 119, p. 75-82, 2015.
- Wang, Fen, Wong, C.S., Chen, D., Lu, X., Wang, Fei, Zeng, E.Y., 2018. Interaction of toxic chemicals with microplastics: A critical review. *Water Res.* 139, 208–219. <https://doi.org/10.1016/j.watres.2018.04.003>.
- Wang, J., Liu, X., Liu, G., 2019a. Sorption behaviors of phenanthrene, nitrobenzene, and naphthalene on mesoplastics and microplastics. *Environ. Sci. Pollut. Res.* <https://doi.org/10.1007/s11356-019-04735-9>.
- Wang, J., Liu, X., Liu, G., Zhang, Z., Wu, H., Cui, B., Bai, J., Zhang, W., 2019b. Size effect of polystyrene microplastics on sorption of phenanthrene and nitrobenzene. *Ecotoxicol. Environ. Saf.* 173, 331–338. <https://doi.org/10.1016/j.ecoenv.2019.02.037>.
- Wang, L., Atkinson, R., Arey, J., 2007. Dicarbonyl Products of the OH Radical-Initiated Reactions of Naphthalene and the C 1 - and C 2 -Alkyl naphthalenes. *Environ. Sci. Technol.* 41, 2803–2810. <https://doi.org/10.1021/es0628102>.
- Wang, Z., Zheng, Y., Zhao, B., Zhang, Y., Liu, Z., Xu, J., Chen, Y., Yang, Z., Wang, F., Wang, H., He, J., Zhang, R., Abliz, Z., 2015. Human metabolic responses to chronic environmental polycyclic aromatic hydrocarbon exposure by a metabolomic approach. *J. Proteome Res.* 14, 2583–2593. <https://doi.org/10.1021/acs.jproteome.5b00134>.
- Wei, C. et al. Occurrence, gas/particle partitioning and carcinogenic risk of polycyclic aromatic hydrocarbons and their oxygen and nitrogen containing derivatives in Xi'an, central China. *Sci. Total Environ.*, v. 505, p. 814-22, 2015.
- Xiang, P., He, R. W., Liu, R. Y., Li, K., Gao, P., Cui, X. Y., Li, H., Liu, Y., & Ma, L. Q. (2018). Cellular responses of normal (HL-7702) and cancerous (HepG2) hepatic cells to dust extract exposure. *Chemosphere*, 193, 1189–1197. <https://doi.org/10.1016/j.chemosphere.2017.11.123>

- Yang, S., Zhao, D., Zhang, H., Lu, S., Chen, L., Yu, X., 2010. Impact of environmental conditions on the sorption behavior of Pb (II) in Na-bentonite suspensions. *J. Hazard Mater.* 183, 632–640. <https://doi.org/10.1016/j.jhazmat.2010.07.072>.
- Yu, H., Yang, B., Waigi, M.G., Peng, F., Li, Z., Hu, X., 2020. The effects of functional groups on the sorption of naphthalene on microplastics. *Chemosphere.* 261, 127592. <https://doi.org/10.1016/j.chemosphere.2020.127592>.
- Zhao, G., Li, J., Wang, X., 2011. Kinetic and thermodynamic study of 1-naphthol adsorption from aqueous solution to sulfonated graphene nanosheets. *Chem. Eng. J.* 173, 185–190. <https://doi.org/10.1016/j.cej.2011.07.072>.
- Zhao, L., Rong, L., Xu, J., Lian, J., Wang, L., Sun, H., 2020. Sorption of five organic compounds by polar and nonpolar microplastics. *Chemosphere.* 257, 127206. <https://doi.org/10.1016/j.chemosphere.2020.127206>.
- Zuo, L.-Z., Li, H.-X., Lin, L., Sun, Y.-X., Diao, Z.-H., Liu, S., Zhang, Z.-Y., Xu, X.-R., 2019. Sorption and desorption of phenanthrene on biodegradable poly(butylene adipate co-terephthalate) microplastics. *Chemosphere.* 215, 25–32. <https://doi.org/10.1016/j.chemosphere.2018.09.173>.